

UNCLASSIFIED

AD NUMBER
AD863202
NEW LIMITATION CHANGE
TO Approved for public release, distribution unlimited
FROM Distribution authorized to U.S. Gov't. agencies and their contractors; Critical Technology; Jul 1969. Other requests shall be referred to Air Force Armament Lab, Attn: ATRD, Eglin AFB, FL 32542.
AUTHORITY
Air Force Armament Lab ltr, 4 Oct 1972

THIS PAGE IS UNCLASSIFIED

AD 863202

AFATL-TR-69-99

STUDIES ON THE BALLISTIC IMPACT OF COMPOSITE MATERIALS

R. L. SIERADEWSKI

G. E. NEVILL, JR.

C. A. ROSS

E. R. JONES

DEPT. OF ENGINEERING SCIENCE AND MECHANICS
UNIVERSITY OF FLORIDA

TECHNICAL REPORT AFATL-TR-69-99

JULY 1969

DEC 21 1969

This document is subject to special export controls and each transmittal to foreign governments or foreign nationals may be made only with prior approval of the Air Force Armament Laboratory (ATRD), Eglin AFB, Florida 32542.

AIR FORCE ARMAMENT LABORATORY

AIR FORCE SYSTEMS COMMAND • UNITED STATES AIR FORCE

EGLIN AIR FORCE BASE, FLORIDA

Best Available Copy

Best Available Copy

STUDIES ON THE BALLISTIC IMPACT OF
COMPOSITE MATERIALS

R. L. Sierakowski

G. E. Nevill, Jr.

C. A. Ross

E. R. Jones

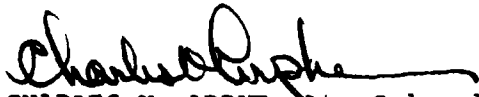
This document is subject to special export controls and each transmittal to foreign governments or foreign nationals may be made only with prior approval of the Air Force Armament Laboratory (ATRD), Eglin AFB, Florida 32542.

FOREWORD

This final report documents research accomplished during the period 17 June 1968 to 16 June 1969 by the Department of Engineering Science and Mechanics of the University of Florida, Gainesville, Florida, under Contract F08635-68-C-0115 with the Air Force Armament Laboratory, Eglin Air Force Base, Florida. Mr. L. L. Wilson (ATRD) was program monitor for the Armament Laboratory.

Information in this report is embargoed under the Department of State International Traffic in Arms Regulations. This report may be released to foreign governments by departments or agencies of the U. S. Government subject to approval of the Air Force Armament Laboratory (ATRD), Eglin AFB, Florida 32542, or higher authority within the Department of the Air Force. Private individuals or firms require a Department of State export license.

This technical report has been reviewed and is approved.



CHARLES K. ARPKE, Lt. Colonel, USAF
Acting Chief, Technology Division

ABSTRACT

The dynamic compressive behavior of unidirectional composites consisting of representative continuous and discontinuous filament reinforced specimens has been investigated. Principal emphasis has been placed on a steel-epoxy system for which a fabrication procedure yielding specimens of high quality and consistency has been developed. Tests at various strain rates were conducted using a conventional Tinius Olsen machine and a Split Hopkinson Pressure Bar System. Results indicating the influence of volume fraction of reinforcing material in the steel-epoxy specimens on strain rate sensitivity are obtained. The apparent existence of a transition region in strain rate sensitivity as the volume percent of reinforcement increased has been noted. Evidence has also been obtained on the mode of failure for the steel-epoxy specimens as a function of strain rate and volume percent of reinforcement. For the Al-Al₃Ni specimens a shear mode failure based on rotation and lateral motion of the 'discontinuous' reinforcements was observed while the fiberglass specimens exhibited a brush-like failure. The failure characteristics of composites under low velocity impact were studied using an air gun assembly developed under this program. A simple method of predicting failure modes and critical velocities from the strain rate data is proposed for the steel-epoxy specimens. Comparisons of the theoretical predictions with experimental results show good agreement. Further correlation of the terminal ballistics behavior of composite projectiles with their dynamic properties has been obtained from photographic recordings of the impact event.

This document is subject to special export controls and each transmittal to foreign governments or foreign nationals may be made only with prior approval of the Air Force Armament Laboratory (ATRD), Eglin AFB, Florida 32542.

TABLE OF CONTENTS

Section	Page
I Introduction.	1
II Technical Background.	4
III Materials and Procedures.	13
IV Results and Discussion.	28
V Conclusion.	64
References.	66

LIST OF FIGURES

Figure	Title	Page
1.	Mandrel and Wire Spacing Apparatus	15
2.	Complete Winding Machine	17
3.	Fabricated Test Specimens - 10% Volume of 0.016 dia. wire	19
4.	Fabricated Test Specimens - 10% Volume of 0.008 dia. wire	20
5.	Fabricated Test Specimens - 10% Volume of 0.004 dia. wire	21
6.	Air Gun Assembly and Related Equipment	24
7.	Muzzle Velocity vs. Chamber Pressure Calibration	26
8.	Muzzle Velocity vs. Projectile Diameter	27
9.	Stress-Strain Curves for Steel-Epoxy Composites $V_f = 10\%$ Wire Dia. = 0.004 in.	29
10.	Stress-Strain Curves for Steel Epoxy Composites $V_f = 10\%$ Wire Dia. = 0.008 in.	30
11.	Stress-Strain Curves for Steel-Epoxy Composites $V_f = 10\%$ Wire Dia. = 0.016 in.	31
12.	Stress-Strain Curves for Steel-Epoxy Composites $V_f = 26\%$ Wire Dia. = 0.008 in.	32
13.	Stress-Strain Curves for Steel-Epoxy Composites $V_f = 26\%$ Wire Dia. = 0.016 in.	33
14.	Critical Strain vs. Strain Rate for Steel-Epoxy Composites $V_f = 10\%$	34
15.	Critical Strain vs. Strain Rate for Steel-Epoxy Composites $V_f = 26\%$	35
16.	Stress vs. Strain Rate with Varying Strain Steel- Epoxy Composites $V_f = 10\%$ Wire Dia. = 0.004	37

LIST OF FIGURES (CONTINUED)

Figure	Title	Page
17.	Stress vs. Strain Rate with Varying Strain Steel-Epoxy Composites $V_f = 10\%$ Wire Dia. = 0.008 in.	38
18.	Stress vs. Strain Rate with Varying Strain Steel-Epoxy Composites $V_f = 10\%$ Wire Dia. = 0.016 in.	39
19.	Stress vs. Strain Rate with Varying Strain Steel-Epoxy Composites $V_f = 26\%$ Wire Dia. = 0.008 in.	40
20.	Stress vs. Strain Rate with Varying Strain Steel-Epoxy Composites $V_f = 26\%$ Wire Dia. = 0.016 in.	41
21.	Maximum Stress vs. Strain Rate Steel-Epoxy Composites	42
22.	Steel Epoxy Composites - Failure Modes	43
23.	Dynamic Stress-Strain Curve	
	(a) Epoxy - $V_f = 0\%$	44
	(b) $V_f = 10\%$ Wire Dia. = 0.004 in.	44
	(c) $V_f = 10\%$ Wire Dia. = 0.008 in.	45
	(d) $V_f = 10\%$ Wire Dia. = 0.016 in.	45
	(e) $V_f = 26\%$ Wire Dia. = 0.008 in.	46
	(f) $V_f = 26\%$ Wire Dia. = 0.016 in.	46
24.	Stress-Strain Curves, Fiberglass Composite	48
25.	Critical Strain vs. Strain Rate, Fiberglass Composite	49
26.	Maximum Stress vs. Strain Rate, Fiberglass Composite	50
27.	Stress vs. Strain Rate with Varying Strain, Fiberglass Composite	51
28.	Fiberglass Composites - Failure Mode	52
29.	Dynamic Stress-Strain Curve for Fiberglass Composite	52
30.	Stress-Strain for Aluminum Nickel Composite	54

LIST OF FIGURES (CONCLUDED)

Figure	Title	Page
31.	Stress vs. Strain Rate for Aluminum Nickel Composite	55
32.	Dynamic Stress-Strain Curve for Al-Ni Composite	55
33.	Critical Fracture Velocity vs. Wire Diameter for Steel-Epoxy Composites $V_f = 10\%, 26\%$	57
34.	Critical Plastic Flow Velocity vs. Wire Diameter for Steel-Epoxy Composites $V_f = 10\%, 26\%$	57
35.	Dynamic Deformation at Various Impact Velocities Steel-Epoxy Composites $V_f = 10\%$, Wire Dia.=0.016in.	59
36.	Dynamic Deformation at Various Impact Velocities Steel-Epoxy Composites $V_f = 26\%$, Wire Dia.=0.016 in.	60
37.	Dynamic Fracture Behavior of Composites	62
38.	Aluminum-Nickel Composites Failure Behavior	63

LIST OF TABLES

Table	Title	Page
I	Selected Types of Filament/Whisker Reinforced Composites	13
II	Filament Spacing for Volume Percent and Wire Diameter	14
III	Critical Velocities for Steel-Epoxy Composites	58

SECTION I

INTRODUCTION

In recent years, the design limitations imposed by conventional monolithic materials plus the potential value of composite materials as improved high-strength structural elements have led to great interest in composites. At present, however, there exists only a limited body of knowledge of the basic static and dynamic properties and failure behavior of such materials to support rational design for various service conditions. Nevertheless, the promise remains high with the limited analytical and experimental evidence available indicating that through the emerging interdisciplinary approach to materials technology, improvements in weight and cost effectiveness using composite materials should be of extreme importance in the future. This has been emphasized and recognized by the Air Force in their examination of the role of composite materials technology during the next two decades [1]. Indeed, the rapidly expanding technology of multiphase materials indicates their great potential as tomorrow's super materials.

Of the various types, fiber reinforced composites of both the continuous and discontinuous type appear to be of primary interest to engineers concerned with structural applications. The development of these materials requires new techniques for understanding and evaluating the basic material properties of the constituents individually and their performance in composite systems. This is fundamentally important since new design considerations demand improved analytical models and experimental data in order to fully exploit the potential of such materials.

As in other areas, the use of composite techniques to custom design materials for particular service and mission requirements in the projectile and ballistic impact area appears promising. Thus, it appears that the important material properties associated with the terminal ballistics problem, notably hardness, durability, toughness, strength, could be optimized by suitable selection of composite type and constituents. However, with the use of composites, a new class of materials, the meaning and significance of basic materials properties may be changed and require re-evaluation in the light of the unique characteristics of composite materials. For example, the property material hardness, which usually is measured by indentation tests, and is a commonly used parameter for determining material suitability for ballistic design, becomes less identifiable, and significant for a composite material.

The situation outlined led to the present effort. Broadly speaking, the goal of the effort has been to provide basic data on the dynamic properties and fracture characteristics of representative composite materials which contribute to the evaluation of their suitability and potential for various terminal ballistics-oriented missions. Thus, this program emphasized the terminal ballistics problem and the specific interaction between projectile and target.

In the terminal ballistics problem the impact between projectile and target produces complex dynamic stress states. These stress states change rapidly with time, and a given material element is likely to be subjected to compression, tension and shear stress during impact. Clearly no one material or design can optimize performance under all of these load combinations. However, by utilizing the flexibility inherent in the composite material concept, significant improvements over the performance of monolithic materials should be possible.

Due to their promise and state of development the filamentary and whisker reinforced subclass of composite materials was chosen for investigation. The reinforcing elements considered have been both of the continuous and discontinuous type, placed in organic and inorganic matrix systems.

The dynamic and fracture mechanics aspects of the impact problem are interrelated, in that knowledge of the dynamic material properties and of wave propagation are essential elements for predicting crack initiation and propagation, spalling and associated phenomena. Thus, in order to determine fundamental dynamic fracture characteristics of composites, it is advantageous to choose experimental geometries of considerable simplicity. For this reason in the present investigation cylindrical geometry specimens with uniform axial fiber reinforcement have been selected for study.

The present program has sought to systematically evaluate the dynamic deformation and fracture behavior of several representative whisker and filament reinforced composites. The reinforcing elements selected were of discontinuous and continuous type in representative organic and inorganic matrices. The particular composites studied were steel reinforced epoxy, fiberglass reinforced polyester, aluminum nickel reinforced aluminum, and tungsten reinforced copper. Geometrical variations among specimens included variable fiber diameter, fiber spacing and volume percent of reinforcement. Included in the results is a qualitative description of the fracture phenomena based on visual observation of the impact of composite projectiles with targets.

The experimental program involved low strain rate compression testing (in the order of 10^5 to 10^{-1} in/in/sec) using a Tinius Olsen Testing Machine and high strain rate testing (in the order of 10^3 in/in/sec) conducted with a Split Hopkinson Pressure Bar system. For the ballistic impact testing program, an air gun assembly has been fabricated and composite projectiles fired at a massive elastic target. High speed photographs using an image converting camera have been used to provide a visual observation of the dynamic delamination and fracture characteristics. Specific results of the program include qualitative information on the nature and character of the dynamics fracture plus quantitative evaluation of the influence of strain rate, specimen geometry, reinforcement spacing and density, composite component property relations and estimates of resultant energy to fracture.

SECTION II

TECHNICAL BACKGROUND

This section presents a brief summary of the composite field as it relates to the ballistic impact area and includes representative references to information complementing the present area of investigation.

2.1 Types of Composite Materials

In recent years, the emergence of an interdisciplinary approach to materials technology has resulted in a new emphasis on the potential value of multiphase materials as improved structural elements [2-9]. Often in the past, work on composite materials has been rather specific and narrow, primarily because of limited structural interest and a lack of communication of information on particular composite developments. With the current laboratory developments of selected high-performance types of reinforcing members, the conventional limitations of monolithic materials has been further emphasized. Thus far in the emergent technology of composite materials, primary concern has been in applying the appropriate constituent materials in such a manner as to meet specific design, economic and service conditions.

A problem which arises concerns the definition of a composite material. Any monolithic material may be considered as a composite material at a particular level of structural modeling. From a mechanistic viewpoint, that is, a macroscopic level, the interest is in large structural forms with constituents such as particles, flakes, filaments and whiskers, as reinforcing elements. Considering the above remarks, the definition as posed in [10] is appropriate.

"A composite material is a material system composed of a mixture or combination of two or more macroconstituents that differ in form and/or material composition and that are essentially insoluble in one another."

The above definition establishes the variables necessary to clarify the useful forms of structural composites.

Essential to this understanding is knowledge of the constituent members which form the composite materials. The principal constituent forms that are presently available to engineers in developing structural composites are fibers, particles, flakes,

fillers, laminates and matrix materials. The matrix material is the essential bonding constituent which gives the composite its structural shape.

Important to all composites is the bonding force at the interface between reinforcing material and matrix. For artificial composites, that is those composites which are fabricated by placement of the reinforcing element directly into the matrix material. The interface region between fiber reinforcement and matrix is, of course, an area of principal concern. For a composite of the dispersion hardened and eutectic alloy type, the reinforcing element is produced by metallurgical processing, thus, the problem associated with interface bonding becomes a control parameter of the processing technique.

For artificial composites the constituent materials can be inserted in the matrix in two ways. One is a regulated or repeated distribution of the reinforcing phase and the second is an irregular or random distribution of the reinforcing material. The reinforcing materials involved may be either of the continuous or discontinuous type in the modeled system.

The above qualitative descriptions of composite distribution lead naturally to different macroscopic quantitative mathematical modeling. In particular, these material distributions admit the following mathematical models:

- 1) homogeneous-isotropic
- 2) homogeneous-anisotropic
- 3) nonhomogeneous-isotropic
- 4) nonhomogeneous-anisotropic

For particular classes of composites each of the above macroscopic models may provide a suitable quantitative description for analytical purposes. For example, in considering monolithic materials we can assume the material to be homogeneous and isotropic. This is permissible since the level of mathematical modeling is macroscopic and the statistical distribution of grains is unordered. On the other hand, for materials possessing a gradient in the distribution of reinforcing elements, the material may be considered nonhomogeneous and isotropic. Another permissible model occurs if the material of the reinforcing phase is placed in an irregular but oriented manner, as for example in a unidirectional way. The composite may then be modeled as being homogeneous and anisotropic. A combination of either of the latter two types of composites leads to a mathematical model which is nonhomogeneous and anisotropic.

The types of composites that are available for structural members fall into three broad classes. These general classes are:

- 1) Laminar composites, consisting of layered or laminar constituents, including sandwich type materials.
- 2) Particulate, flake like, and skeletal composites. Included in this group may be skeletal matrix materials, dispersion strengthened materials and materials which may or may not have appropriate binding matrices.
- 3) The fiber reinforced composites consisting of discontinuous or continuous fibers with or without an appropriate binding matrix.

The behavior of these composites depends on the overall constituent properties of the reinforcing phases and on such geometrical quantities as shape and arrangement of constituents and the interaction between the constituent and binding matrix. Clearly, compared to monolithic materials, there are a larger number of degrees of freedom of the system, necessitating specification of many parameters in order to establish overall material response. However, it is just this high level of flexibility and freedom which permits great versatility in ultimate material design and performance.

Prediction of composite behavior may be based on several assumed constituent interaction modes. One method is to consider the individual contributions of each of the constituents in a summation fashion. That is, the ultimate behavior of the composite is projected by individually adding the performance characteristics of the reinforcing and bonding phases. Another approach is to consider that the individual elements complement each other in predicting the overall material response. Such materials may use one phase for one type of performance while the other phase may be utilized for another service condition. An example of such a system is a clad material in which the thin surface layer may be selected for electrical characteristics while the interior metal is used as a structural load carrying material. The third possible approach results from considering the constituents as supplementing the individual material properties of other constituents. For this type composite, mechanical properties can be obtained which are different than those of either of the constituent materials.

The most important of the above mentioned composites, which has received considerable attention in recent years, is the fiber reinforced type. The ultimate promise of such materials for high performance structural elements is presently being developed. In this discussion only those fiber-type composites which have a binding matrix are considered, thus omitting textile-type materials.

Many factors contribute to the performance of fiber matrix composites. Some of the most important of these are fiber orientation, length (continuous or discontinuous filaments) shape (circular, rectangular, etc.), material of the fibers, properties of the matrix and the structural integrity of the bond between the reinforcing phase and the matrix material. Bond performance, in turn, is dependent on chemical compatibility, mechanical compatibility due to stresses resulting from difference in thermal expansion of the two phases, absorption characteristics and fiber-matrix solubility as well as other factors.

In the development and application of fiber composites, it is useful to distinguish and classify the types which have been fabricated to date. For purposes of discussion, the following four broad classifications can be considered as basic to fibrous composites.

- 1) Organic fiber - organic matrix (example, automobile tires)
- 2) Inorganic fibers - organic matrix (example, glass reinforced plastic)
- 3) Inorganic fibers - inorganic matrix (example, tungsten-copper system)
- 4) Organic fibers - inorganic matrix (example, graphite ceramic materials)

The above remarks serve as an introduction to the classification and understanding of composites, in general and some of the more important composites presently being investigated.

2.2 Composite Materials Fabrication

In the fabrication of artificial composites by incorporating reinforcing filaments and/or whiskers manually into organic and inorganic matrices, attention should be given to the selection of reinforcements with minimum chemical degradation, maximizing filament loading efficiency. To achieve these aims, several techniques are available for fabricating such composites. In general,

great reliance must be placed on the extent and limitations imposed by the chemical and mechanical bond problems. Some of the techniques which have been successfully used to fabricate multiphase composites are listed below and details can be found in [2-7] [11-33]. A brief summary of the principal techniques presently being used is included below.

Filament Impregnation - In this process, a series of wire bundles is impregnated with an appropriate binder material. The system is formed by winding filaments on a mandrel assembly in order to insure proper spacing and separation of the individual columns and layers of reinforcing elements. The mandrel assembly is then immersed into an appropriate liquid binder and the system allowed to furnace cool following a programmed procedure. In this way it is possible to form continuous and discontinuous metal and non-metal matrix reinforced systems.

Vacuum Infiltration - This technique utilizes bundles of filaments which are passed through an appropriate liquid metal bath in which the individual filaments are wetted as they pass through the bath assembly. Upon removal of the bundles of filaments the excess material is removed. Composites with high volume fractions of reinforcing constituents have been formed in this particular manner. This technique appears suitable for lower melting temperatures of matrix materials but at higher temperatures a potential danger exists in deterioration of fiber properties and reaction between the reinforcing phase and matrix material.

Electrodeposition - The electrodeposition technique utilizes a conducting material (cathode), which also acts as a supporting member, immersed in an electrolytic bath. An anode is located a short distance from the support member and a potential difference applied between cathode and anode. Filaments for the resulting composite are wound onto the mandrel and a layer of the anode material is deposited on the mandrel, forming the required composite. The required volume fraction of fiber-matrix ratio is controlled by the rate of deposition of binder material and compatibility of thermal coefficients of potential fiber-matrix materials.

Powder Metallurgy - In this technique whiskers or chopped fibers are selected as reinforcing materials. These materials are then mixed with an appropriate powder matrix and either hot or cold pressed under high pressure to consolidate the matrix material. Some of the fabrication problems which must be considered in using this technique are applying pressures such that breakup of individual whiskers or fibers does not occur, elimination

of porosity effects in the subsequently formed matrix, and the alignment problem of orienting the whiskers or chopped fibers in an appropriate manner.

In situ growth - In this technique a cylindrical sample is drawn through a controlled thermogradient producing a unidirectionally solidified sample. This process produces a reinforcing phase which does not depend upon man-made handling and fabricating techniques but incorporates the essential advantages of chemical and mechanical bonding in a systematic manner.

Coextrusion - In this method combined elements of constituents are passed through appropriate dies producing an extrusion consisting of reinforcing phase and matrix material. Sheet wire forms have been obtained in this particular manner.

Casting - In this technique single fibers or bundles of fibers are appropriately cast through a molten metal bath. The amount of material deposited upon the filaments being passed through the molten bath is controlled by the speed in which the fiber is processed. In this way a regulated and continuing deposition of matrix material can be formed on the appropriate fiber arrangement. The filaments produced in this manner are then consolidated to form the resultant composite material.

Plasma Spray Technique - In this technique a series of fibers is wound upon a rotating mandrel assembly and the binding material is deposited on the fibers by plasma spraying the matrix material directly onto the mandrel assembly. A second layer of wires is then wound and the spraying technique repeated again. In this way a continuous composite material is formed with numbers of layers depending upon the desired thickness and resultant design properties.

Diffusion Bonding Method - In this technique the appropriate layers of filament materials are rewound and infiltrated in desired thicknesses with matrix material is then subjected to combinations of high pressure and plastic deformation to yield the desired composite structural shape. One of the interesting features of this technique is that it is commercially adaptable and provides use of alternate layers of matrix sheet and material properties.

Some of the other useful techniques that have been used in forming composites are rolling, vapor deposition, and pneumatic impaction.

2.3 Composite Dynamic Materials Properties

In evaluating the performance characteristics of inorganic and organic matrix systems many factors may be influential in determining the overall material response. Some factors which can be cited are, constituent mechanical properties, chemical and mechanical bonding of constituent and matrix, and such geometrical properties as size, shape, and orientation of reinforcements. In addition, the influence of crack initiation and propagation through both continuous and discontinuous reinforced composite behavior. The ultimate objective of such investigations is to predict from a micromechanical model the overall system performance. This implies an understanding and ability to project composite performance from the individual constituent properties.

For non-metal matrix composites stress analysis procedures presently consider the constituent reinforcing phase and the matrix phase as elastic-plastic [35-56]. A refinement of these principles to include the visco elastic-plastic non-metal matrix system has been obtained in [57-60]. Both linear and nonlinear response of such systems has been considered in the analytical predictions.

It is known that the essential features of the static analysis can be extremely useful in studying dynamic properties. However, the dynamic influences are often of an entirely different nature and such properties as measured in terms of mechanical properties, and failure modes may be significantly different from static behavior. Investigations into such dynamic properties for composite materials considering both analytical and theoretical work, have been of recent interest. Since the dynamic properties evaluation and wave propagation phenomena are interrelated in that one requires a prior understanding of the other, interests in both is of importance for understanding multi-phase material behavior.

A general survey of the ballistic impact area is included in [61]. To obtain information on dynamic properties from analytical investigations, some work has been done on wave propagation in stratified media in the geophysics and geological areas [62-65]. Further work on layered homogeneous and non-homogeneous elastic media is contained in [62-72]. For materials of an anisotropic nature, references [73-75] provide information on analytical investigations of wave propagation phenomena. In general, such analytical results suggest possible control of the spalling and fragmentation problem, depending upon the material reinforcing layers, types of material, thickness of material,

and other important properties. The effect of wave reinforcement and dispersion on wave propagation in fiber-reinforced composites has been treated to some extent in [75-79]. These results continue to prove encouraging and suggest the potential use of such composites for controlling spall and fragmentation. To experimentally explore some of the dynamic properties of materials, several symposia have been devoted to such studies for monolithic materials, [80-82].

One of the more useful tools for studying such dynamic properties has been the Split Hopkinson Pressure Bar [84-87]. This device has been used to study the dynamic mechanical properties of conventional engineering materials and more recently extended to include time-dependent materials as well [88]. Application of this technique to composite materials is quite limited and the results presented in this report add appreciably to the body of data available. Some experimental results using this system are reported on metal powder-epoxy systems in [89]. In addition to the Hopkinson Pressure Bar some experimental work on dynamic compressive properties of potential matrix materials is reported on in [90].

A limited study of the wave propagation and dynamic modulus measurements of fibrous and particle reinforced composite materials has also been used recently and good correlation with analytic predictions have been achieved in [94-96].

2.4 Composite Failure Dynamics

The development of analytical and experimental tools to investigate the impact-fracture dynamics of monolithic materials has progressed at an increasing rate in recent years. Some basic references on this subject are included in [97-100].

As in the case of dynamic material properties, the impact-fracture dynamic characteristics of fiber reinforced composites are only of recent interest and investigation. For the case of static failure, some work which has been done in this area for continuous and discontinuous fiber composites is cited in [101-108]. Some of the important failure characteristics are filament debonding, filament buckling (microinstability), filament sliding, filament fracture, shear buckling (combination of matrix shear and fiber buckling), and associated phenomena. All the above elements play an important role in predicting failure behavior of continuous and discontinuous composites under quasi-static loads. In addition, the important parameter of critical fiber length to diameter becomes significant in determining failure and reinforcing action of fibers [101].

The limited data available on dynamic and impact phenomena indicate that laminar composites have potential usefulness as high energy absorbing materials based on the ability of the material to restrain crack propagation by its oriented nature [109]. Studies on fiberglass reinforced plastic have been conducted and the penetration resistance of such materials found to be high based on their weight efficiency as compared to steel in stopping small caliber projectiles [110]. An extension of this concept to ceramic and plastic composites has proven useful for lightweight armor systems [111-114]. A further discussion of the potential usefulness of ceramic materials in armor systems, including performance characteristics, correlation studies of important material properties, and optimization characteristics is discussed in [115-122]. Other dynamic failure studies have been made on the deformation properties of skeletal composites in [123]. In addition, impact fracture characteristics in filament reinforced tank materials have been studied by [124], and comparison with conventional materials made. Some additional studies conducted at very high impact velocities on conventional stainless steel materials with composite reinforcements have been reported on in [125].

At the present time the use of composite materials in dynamic applications can be characterized as a rapidly developing field of great promise but severely limited by the paucity of basic information on the dynamic materials properties and fracture behavior of material of maximum interest.

SECTION III

MATERIALS AND PROCEDURES

This section deals with materials selection, fabrication, and testing methods.

3.1 Materials Selection and Fabrication

The types of filamentary composite materials selected for this work are shown in Table I.

TABLE I. SELECTED TYPES OF FILAMENT/WHISKER REINFORCED COMPOSITES

Composite Type	Filament/Whisker Type	Matrix Type	Type of Reinforcement
Metal/Non-Metal	Steel Filaments Ductile	Epon 828	Continuous
Non-Metal/ Non-Metal	Glass Filaments Brittle	Polyester Brittle	Continuous
Metal/Metal	Tungsten Filaments Ductile	Copper Ductile	Continuous
Metal/Metal	Al ₃ Ni Whiskers Brittle	Aluminum	'Discontinuous'

Composite Fabrication

In order to conduct these studies, it was necessary to develop the capability for fabricating selected composite systems in the laboratory. This was due to the fact that desired control in representative material samples of size of reinforcing elements, volume percent reinforcement, spacing and geometry was not commercially available for several of the model systems selected for this investigation. Thus, a significant effort has been devoted to producing sample specimens with high degrees of uniformity and reproducibility. The following paragraphs describe the fabrication procedures, as applicable, for the selected composite materials.

3.1.1 Steel Epoxy

The selection of this system for potential investigation was based on the availability of the constituent materials and the

ability to control the material geometry. The steel wire reinforced epoxy composites utilized in this program were fabricated using a winding machine developed specifically for this program. The winding apparatus was designed to produce twenty cylindrical specimens with nominal dimensions of .375 inch diameter by .500 inch length. Specimens were wound for three different wire sizes and two volume percents.

To obtain the desired filament packing for a square array, the volume percent of fiber reinforcement was calculated using

$$V = \frac{\pi D_f^2}{4 s^2} \times 100$$

where D_f is the diameter of the filament or wire and s is the center to center spacing of the wires in a row or column. The spacing can then be obtained in terms of the required volume percent using

$$s = 892 D_f V_f^{-\frac{1}{2}} = \frac{1}{N}$$

where N is the number of filaments per inch.

The above equation was plotted for selected wire diameters given in Table II with the tabulated number of filaments per inch used for the winding machine design.

TABLE II. FILAMENT SPACING FOR VOLUME PERCENT AND WIRE DIAMETER

Wire Dia.	$V_f = 10\%$	$V_f = 26\%$
.004 inches	90.0	144.0
.008 inches	45.0	72.0
.016 inches	22.0	36.0

All wires were wound around a flat mandrel with nominal dimensions of 0.375 by 1.625 by 2.50 inches with 0.125 inch thick end plates. This mandrel and assembly is shown in Figure 1 where it is labeled A. A threaded shaft, labeled B, of 36 threads per inch, was used to guide the filament onto the mandrel. The filament was guided onto the shaft by a pulley, C, which was carried by the shaft. The gears, D, could be changed to provide a wide ratio of mandrel speed to threaded shaft speed, thereby changing the number of filaments per inch. The figure shown displays a system with gears having a 2:1 ratio corresponding to a particular number of wires, wire diameter and volume percent of reinforcement as found in Table II.

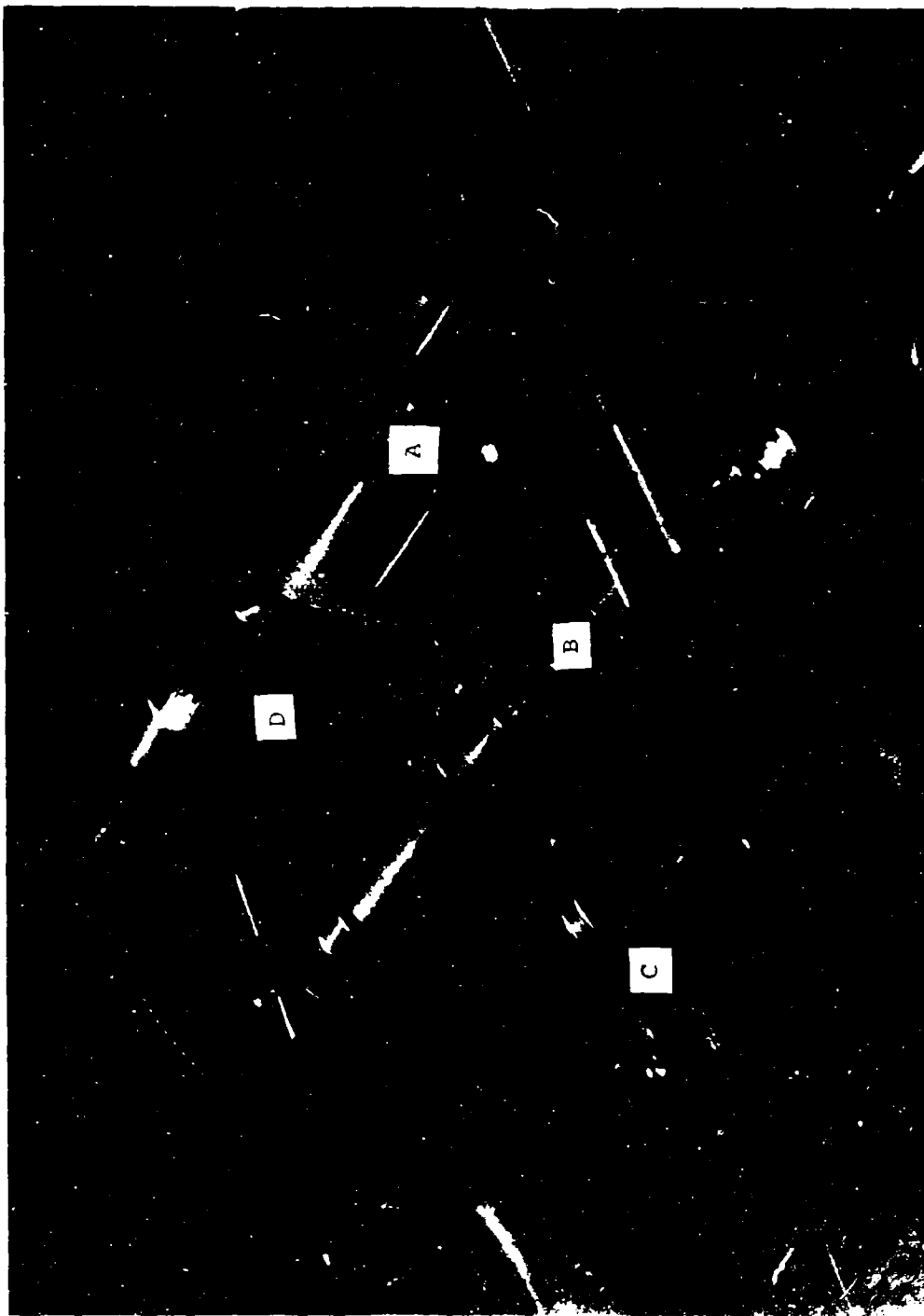


Figure 1 Mandrel and Wire Spacing Apparatus

Figure 2 shows the complete winding apparatus. The mandrel was driven by a 50:1 right angle speed reducer, E, which was powered by a $\frac{1}{2}$ hp electric motor, F, which has a variable speed of 500 to 5000 RPM and a reversing feature. In the left side of the picture is the wire spool, G. Filament tension was controlled by means of a teflon coated cable, properly weighted and wrapped around the pulley, H. The tension was varied through a wide range by adding or removing weights attached to the cable.

The specific winding procedure used was as follows: (a) the mandrel was placed in the winding machine and the guide pulley positioned to place the wire at the end of the mandrel; (b) the wire was secured through a slot in the end plate and the motor turned on to begin winding; (c) wire tension was adjusted to give the maximum possible tension without breakage; (d) after completing the wire layer, the wire was secured at the other end and the motor reversed to reposition the pulley for the next layer; (e) finally, a preformed shim of the correct thickness was placed around the rounded ends of the mandrel in order to provide proper spacing between the filament layers.

Sufficient layers were wound on the mandrel to deposit a depth of filaments of about $\frac{7}{16}$ inches. The mandrel was then removed and cleaned in a trichroethelene vapor degreaser. After cleaning, it was placed in an oven at 150°F for $\frac{1}{2}$ hour to remove all traces of cleaning solvent, and to further prepare the filament assembly for impregnation in the epoxy resin.

The Shell Epon 828 Resin was heated to a temperature of 150°F and mixed thoroughly with 12 parts per hundred of curing agent 400 (formerly curing agent D). The mixture was then de-aired for 15 minutes in a vacuum chamber at 0.6 in. Hg absolute. After raising the vacuum to about 4 in. Hg , the pre-heated mandrel was lowered very slowly into the resin in order to avoid air entrapment. When fully immersed, the vacuum was released, and the resin container with submerged mandrel then removed and placed in an air circulating oven at 150°F . A two-hour time limit was imposed for proper resin cure. The oven heat was then turned off and the resin block allowed to cool slowly to room temperature in order to minimize the effects of thermal shrinkage.

The composite was then carefully cut and sanded out of the resin block. The end plates were removed next, and then the steel mandrel drilled and pressed out. The semi-circular ends, containing the shims, were then cut off leaving two composite blocks about $\frac{7}{16}$ " thick, $1\frac{5}{8}$ " wide and 2" long. These were then cut into six strips, $\frac{7}{16}$ " by $\frac{7}{16}$ " by 2" long, and ground to form dowels $\frac{3}{8}$ " in diameter by 2" long. The dowels were then cut and the ends ground flat and square to give a total of 18 specimens, each

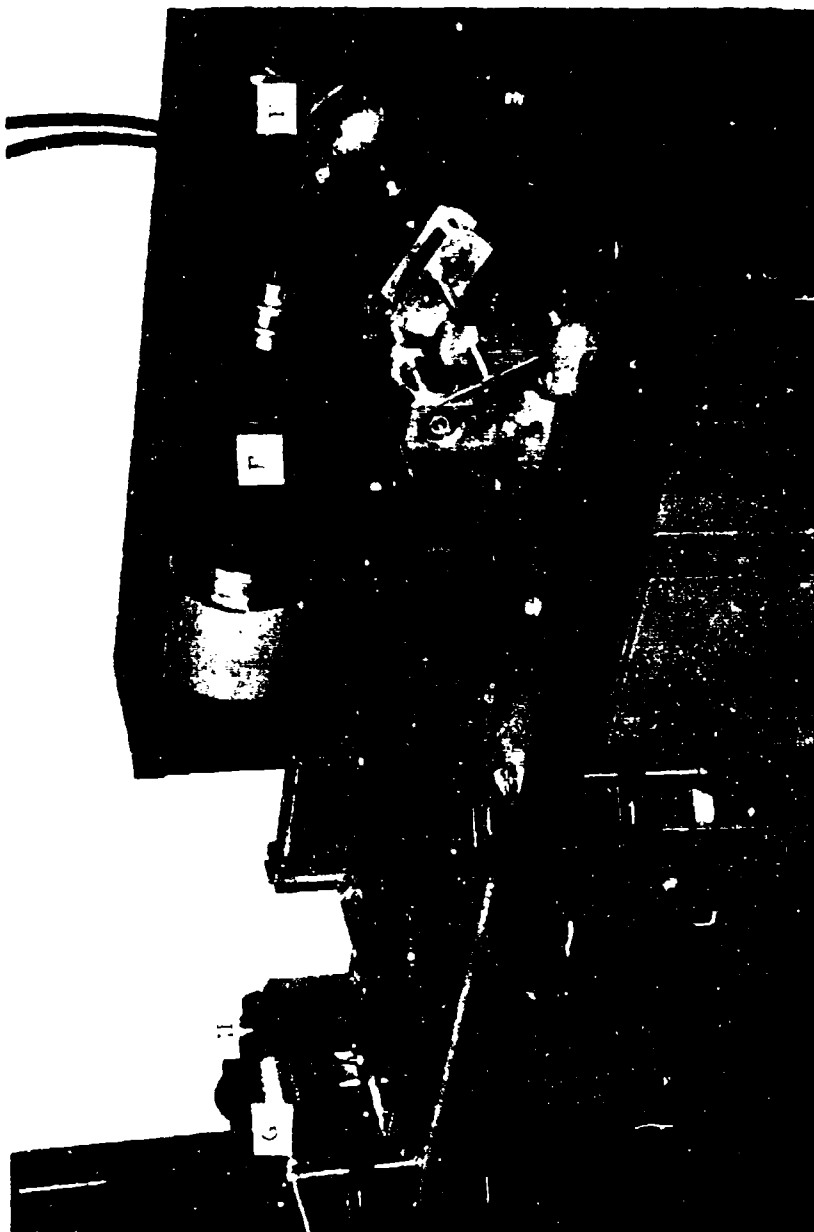


Figure 2. Complete Winding Machine

specimen being 0.375 inches in diameter by 0.500 inches long. Two mandrels were wound for each desired wire size and volume fraction, to give 36 specimens of each selected type. Typical specimens for a ten volume percent composite system with varying wire size are shown in Figures 3 through 5.

3.1.2 Fiberglass

Cylindrical rods of this material, having a diameter of 0.375 ± 0.001 , were purchased from Plastic Rod, Inc. The glass reinforcements represented 61% by volume fraction of reinforcing material and filament diameters were of the order of 0.000037".

3.1.3 Tungsten/Copper

In order to fabricate this system, the method of liquid infiltration was used for casting the specimens. A mandrel of tungsten wire, wound in the manner described for the steel-epoxy system, and pure copper pellets were placed in a graphite crucible. The crucible was placed in a vacuum furnace with maximum operating conditions of 10^{-5} torr pressure at 3100°F . For the specimens fabricated in this program, the crucible assembly was subjected to a pressure of 10^{-6} torr, with no heating for 24 hours. This procedure removed the air from the furnace and prevented oxidation of the tungsten wire at elevated temperatures. The heating element was then used to bring the furnace up to 1500°F in a time of thirty minutes. At this point, the pressure in the furnace chamber was increased to 10^{-3} torr to prevent vapor deposition of the copper on the chamber walls. As the temperature was increased to 2200°F , an inert gas (argon) was used to keep the vapor pressure at 10^{-3} torr. The furnace was held at a temperature of 2200°F and 10^{-3} torr for one hour, and then reduced to 500°F at 10^{-3} torr in four hours. The copper billet was then removed from the crucible for machining.

Time limits made it impossible to obtain specimens of sufficiently high quality to justify testing during the current period. This work will be continued in the next phase of the program.

3.1.4 Aluminum-Nickel

Of the composites selected for initial evaluation in this experimental program, this system is the only one in which the reinforcing phase does not require special design procedures. Indeed, in this composite system the whisker reinforcements are grown in situ in the material during the processing phase. A detailed description of the laboratory procedures for producing

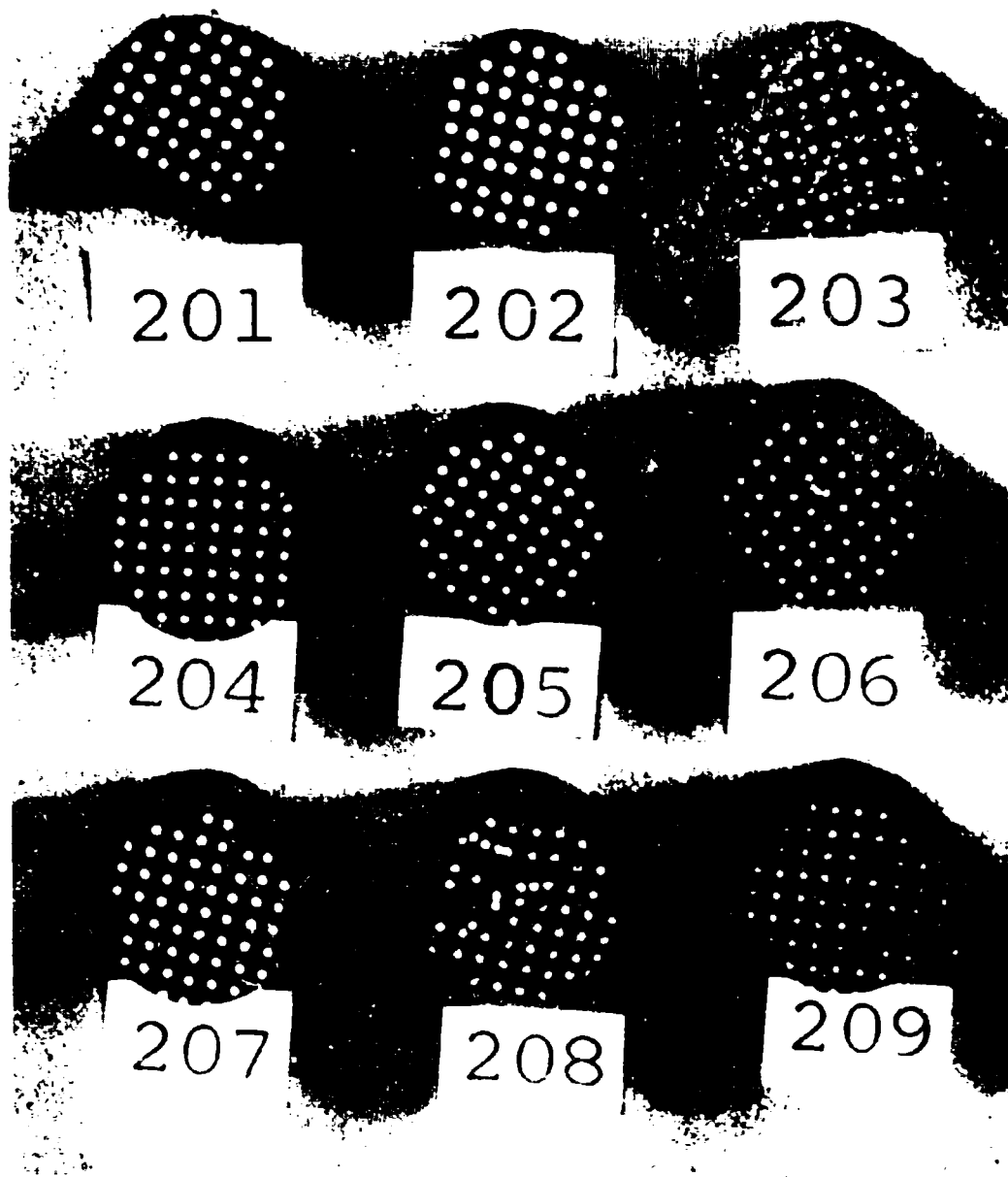


Figure 3. Fabricated Test Specimens - 10% Volume of 0.016 Dia. Wire

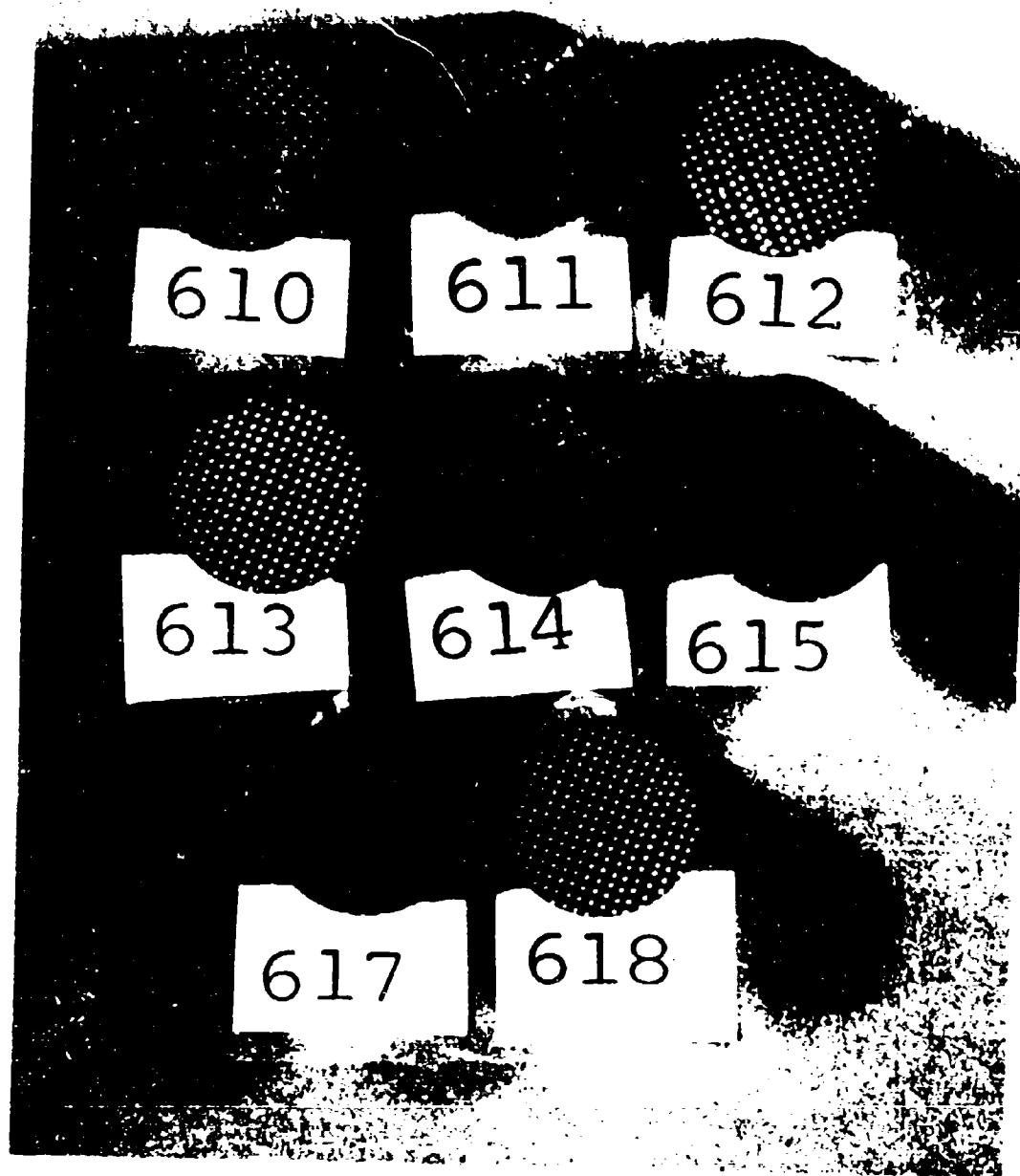


Figure 4. Fabricated Test Specimens - 10% Volume of 0.008 Dia. Wire

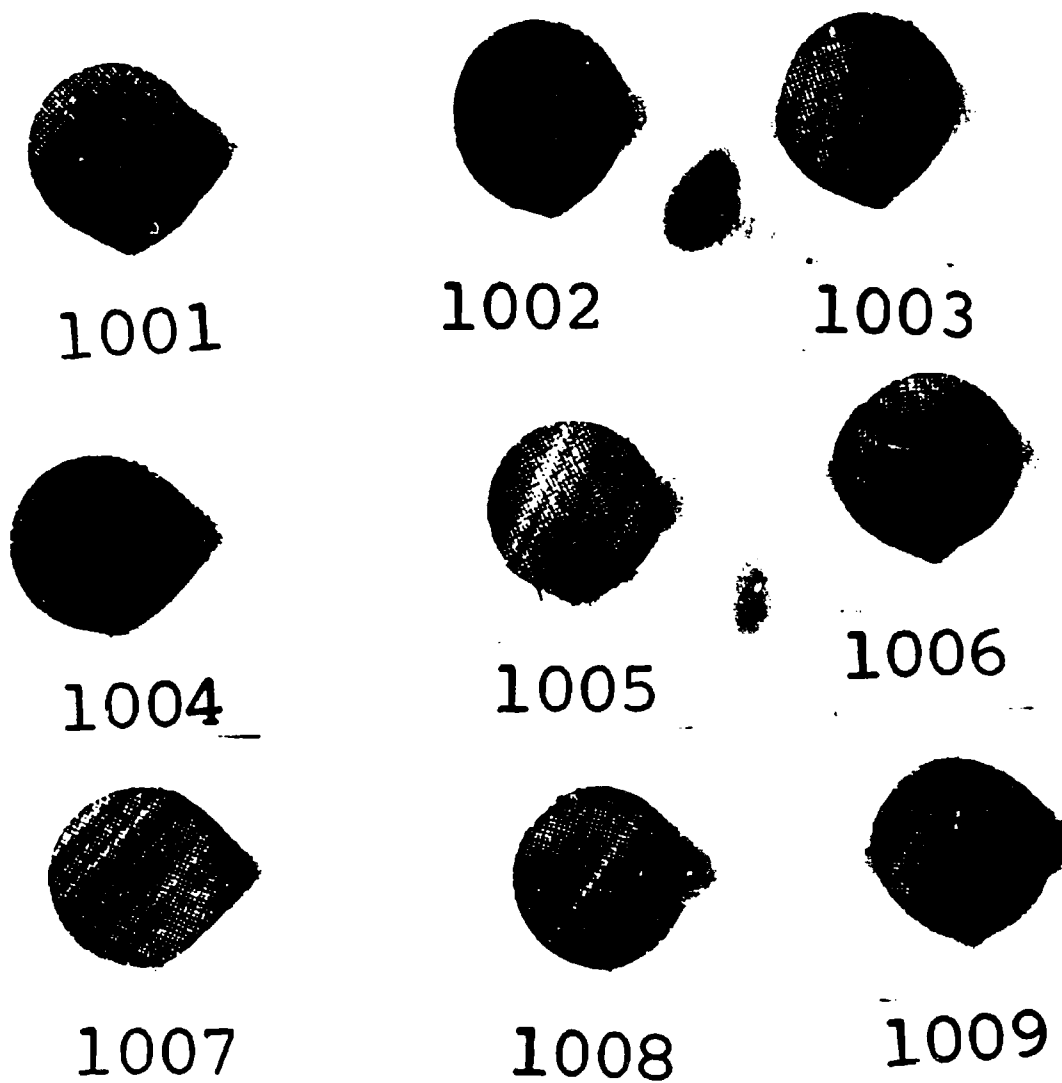


Figure 5. Fabricated Test Specimens - 10% Volume of 0.004 Dia. Wire

this type system is described elsewhere [7]. Briefly, however the method is based on metallurgical observation of unidirectional solidification of single phase alloys. It is known that controlling the heat flow to essentially one direction during the solidification process produces a planar liquid-solid interface. This principle has been applied to eutectic alloy systems resulting in the establishment of a liquid planar interface. The passage of this interface through the melt produces an anisotropic phase mixture with a particular morphology (substructure) consisting of reinforcing whiskers and platelets of approximately micron size.

3.2 Dynamic Materials Properties Testing

The representative fiber and whisker reinforced specimens have been compression tested at varying load and strain rates. The selection of this mode of loading has been dictated by the complementing fracture studies presented elsewhere in this report. The specimens, as used in the test program, have been well lubricated at their end faces with molybdenum disulfide compound in order to minimize end friction.

3.2.1 Tinius Olsen Testing Machine

In order to determine the material response characteristics of the low strain rates (10^{-5} - 10^{-0} in/in/min) a Tinius-Olsen U-Celtronic Testing Machine has been used. In these tests stress (load) is measured by a bonded strain gage load cell and strain measurements are based on the distance between crossheads as determined by an Olsen Type D Deflectometer.

3.2.2 Split Hopkinson Pressure Bar

For examining composite response at the higher strain rates (10^2 - 10^3 in/in/sec) a Split Hopkinson Pressure Bar system has been used. This device, which utilizes measurements of elastic waves in hardened steel pressure bars to determine the relative motion of the two faces of the test specimen and the associated stress, has been described fully by Lindholm [86] and will not be described in detail here.

3.3 Fracture Dynamics Testing

In order to study the fracture failure behavior of the representative composites selected for study, an air gun system modified from that developed in [126] was designed and assembled. The system consists of the following components: the air gun, control panel and related equipment, a velocity measuring system and a high speed photographic system for recording the impact event.

The complete gun system is shown in Figure 6.

The air gun, A, consists of two concentric cylinders having a piston at one end of the inner cylinder serving as a quick acting valve between the outer storage cylinder and the 72-inch long gun barrel, B. In operation, the inner cylinder valve, C, is closed and the inner cylinder pressurized from a storage tank, D. By means of the control panel, E, air is then admitted to the outer cylinder, A. Sudden release of the air from the inner cylinder causes the piston valve to rapidly admit the air stored in the outer cylinder to the barrel and to propel the projectile into the massive target block, F. A movable shield, G, was placed around the target block, F, during testing for safety purposes, as well as to insure capture of the fired projectile. In addition, the non-transparent walls of the shield were lined with styrofoam to minimize secondary damage. All projectiles used in this air gun assembly were muzzle loaded by moving the target block assembly. The air gun was designed for a maximum operating pressure of 2500 psi and has been hydrotested to that pressure, with no observable permanent deformation.

The velocity was determined by measuring the time taken for the projectile to cut two parallel light beams 4.00 inches apart. The light sources, H, emitted light beams through 3/8 inch diameter holes in the scatter shield and were monitored by high gain cells, I. The output of the first two photocells was displayed on a Tektronix Type 549 storage Oscilloscope, J, which was also connected to an electronic counter, K. In use, the counter gives the time in microseconds for the projectile to travel 4.00 inches. The oscilloscope display was used as a check on the counter, for adjustments of light intensity and other checks.

Photographs of the impact events were obtained using a TRW Sub-Microsecond Framing Camera, L. This image converting type camera takes five frames with exposure times from 10 to 200 nanoseconds and interframe delays from 1 to 20 microseconds. A light source and photocell about 1.5 inches from the target were used to trigger a Tektronix Type 556 Dual Beam Oscilloscope, M. The oscilloscope triggered a Honeywell 600 photo flash, N, with zero delay, and then triggered the camera for the first frame after a delay of 20 to 200 microseconds, depending on the velocity of the test. The pictures were recorded on Polaroid film.

Since the oscilloscope delay time had to be set before each test, it was necessary to know the velocity which would be obtained. This was determined by conducting a series of tests at various pressure using projectiles of different weight. A calibration curve was then made from which the velocity could be

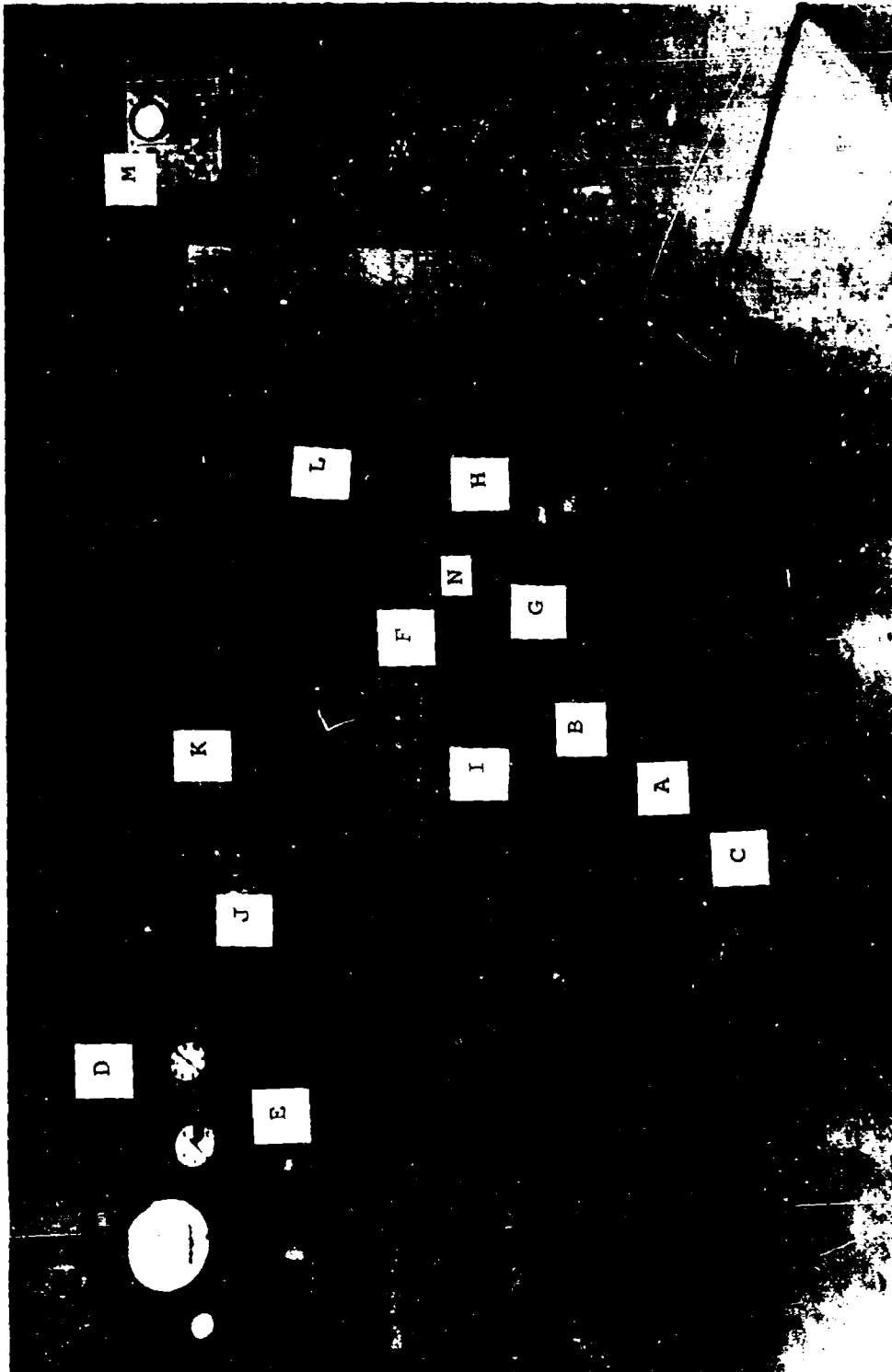


Figure 6. Air Gun Assembly and Related Equipment

accurately predicted. Figure 7 shows the pressure-velocity relationship for projectiles of several different weights and the velocity predicted using the theoretical relationship

$$v = \sqrt{\frac{2PAL}{w}}$$

where v is the velocity, P the outer cylinder pressure, A the area of the projectile, L the barrel length and w the projectile weight. From the figure, it is seen that the above theoretical relationship is inadequate to predict projectile velocity. The experimentally derived curves, however, could be used with an error of less than 2% due to the excellent reproducibility. The discrepancy in the predicted and actual velocity is probably due to neglecting projectile friction, internal losses in the pressurizing air, particularly at the barrel inlet, and air pressure build-up ahead of the projectile as it moved through the relatively long barrel.

The barrel inner diameter for the above mentioned figure was 0.388 inches, while the projectile diameter was 0.375 ± 0.001 . This large clearance was found necessary from a previous series of tests with a barrel of the same length but with a diameter of 0.500 inches. Initial testing with close fitting projectiles showed a prohibitively large velocity scatter for equal pressure tests. A series of aluminum projectiles were, therefore, made having various diameters and tested at a pressure of 400 psi. The results are shown in Figure 8. It is seen that the velocity was strongly dependent on the projectile fit when the projectile diameter was nearly the same as the barrel diameter, and that large scatter resulted. For projectiles 0.013-0.017 inches undersize, however, the velocities were nearly equal and had little variation. An excessively loose fit was found to be a cause of tumbling of the projectile and so a projectile 0.013 inches undersize was used for the composite projectiles tests.

The original barrel with 0.500 inch diameter was designed for use with a sabot and a 3/8" diameter projectile. This technique would increase the maximum velocity obtainable. In practice, it was found difficult to strip the sabot from the projectile at the muzzle without touching or tumbling the projectile. For this reason, and since the velocities required in the present program were easily attainable with a smaller barrel, the 0.388 inch diameter barrel was fabricated and used for the composite projectile tests.

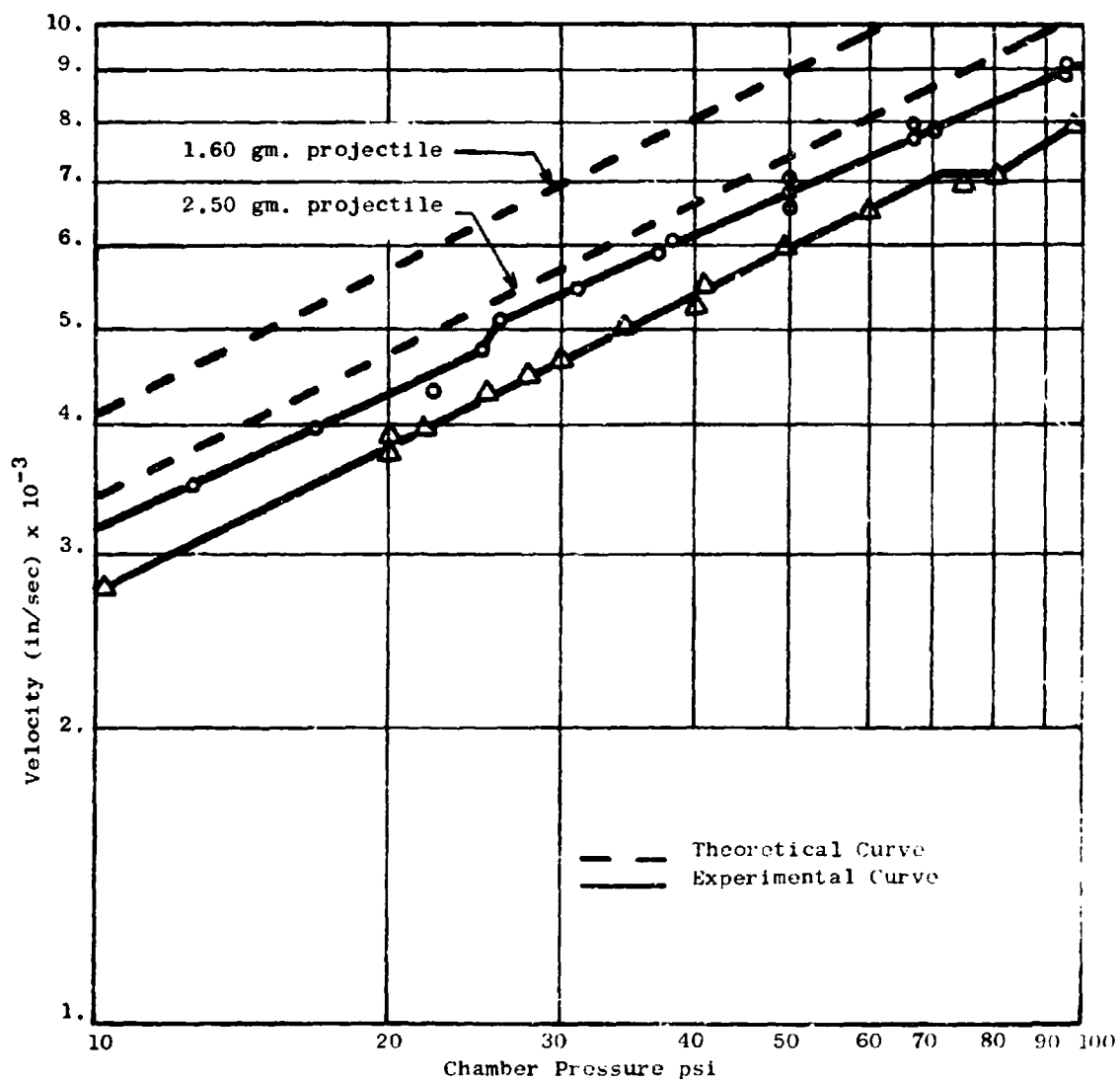


Figure 7. Muzzle Velocity vs. Chamber Pressure Calibration

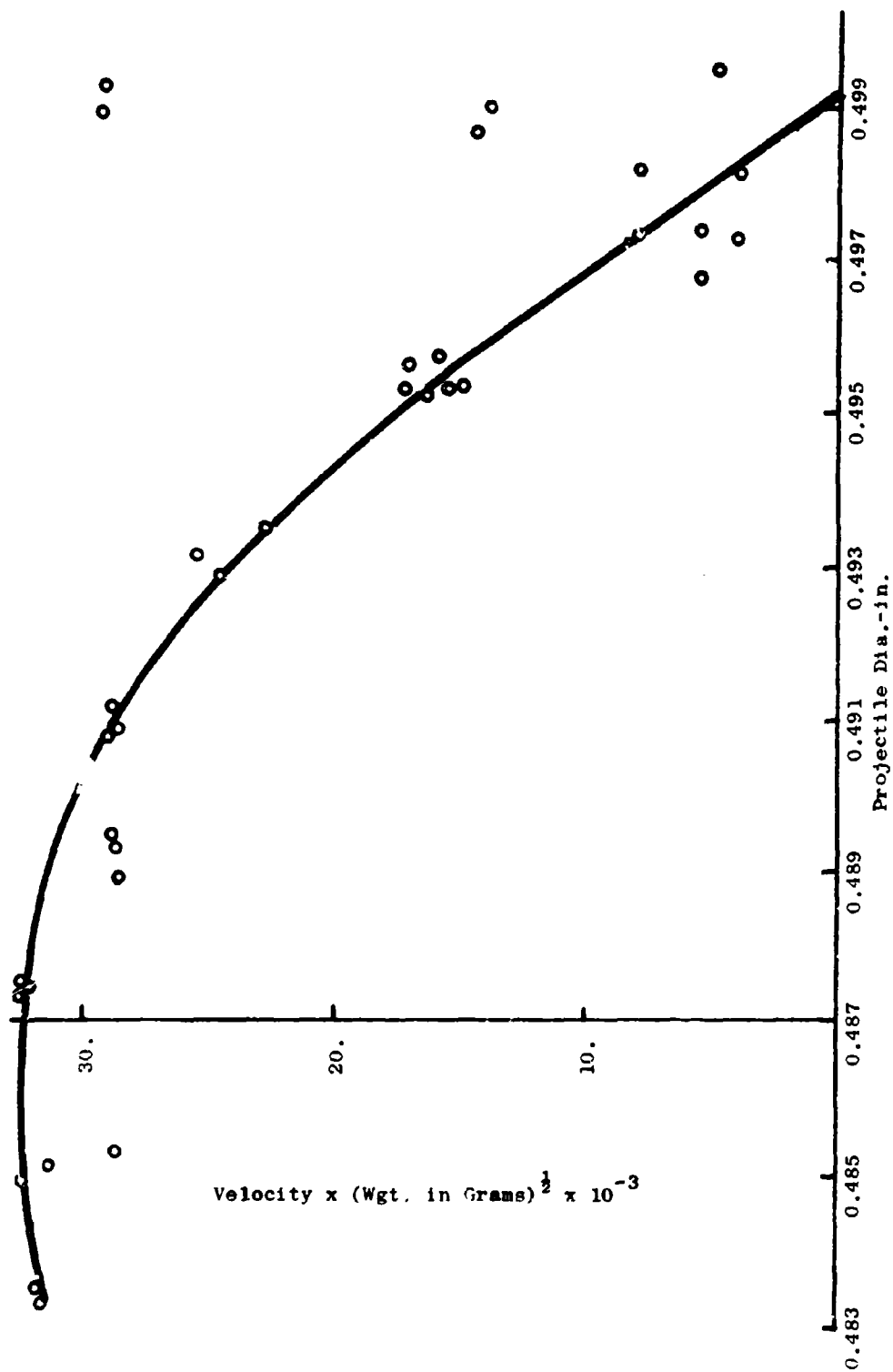


Figure 8. Muzzle Velocity vs. Projectile Diameter

SECTION IV

RESULTS AND DISCUSSION

4.1 Dynamic Compressive Properties

A discussion of results for each of the composite materials tested is presented below.

4.1.1 Steel-Epoxy

A principal part of the present investigation has involved a series of tests on a representative continuous inorganic reinforced organic matrix composite, a steel-epoxy system. This model system was selected for study based on the relative ease of controlling fabrication processing as compared with other systems. For the steel-epoxy series of tests, different reinforcement volume fractions and different wire sizes were selected for optimization and characterization purposes (see Table II). A summary of the appropriate illustrations showing the effects of varying these parameters is shown in Figures 9 through 20. Figures 9 through 13 illustrate the stress-strain characteristics as a function of strain rate with filament size and volume percent reinforcement as parameters. These results represent the average results of several samples tested at each strain rate. It is observed that in each case the smaller wire sizes for corresponding volume fractions of reinforcing material produce higher stress values. Further, as expected, increasing the volume percent of reinforcing filaments leads to higher stress values. The stress increase with decreasing filament size is attributed to the greater amount of surface bonding area between filament and matrix. In addition, it is also noted that for a constant volume fraction there appears to be an optimum wire size for maximum reinforcing action.

In this sequence of curves (Figures 9 through 13), several curves have closed points associated with the plotted data. These points represent selected points of horizontal tangency and thus of maximum stress on the stress-strain diagram. In the other cases the specimens were not deformed to sufficiently large strain to reach a maximum stress and a strain reversal and associated horizontal tangent. The strain associated with this stress maximum is here denoted the critical strain.

Figures 14 and 15 are plots of critical strain versus corresponding strain rate, with filament size a parameter for constant volume percent of reinforcing fiber. These data were obtained by

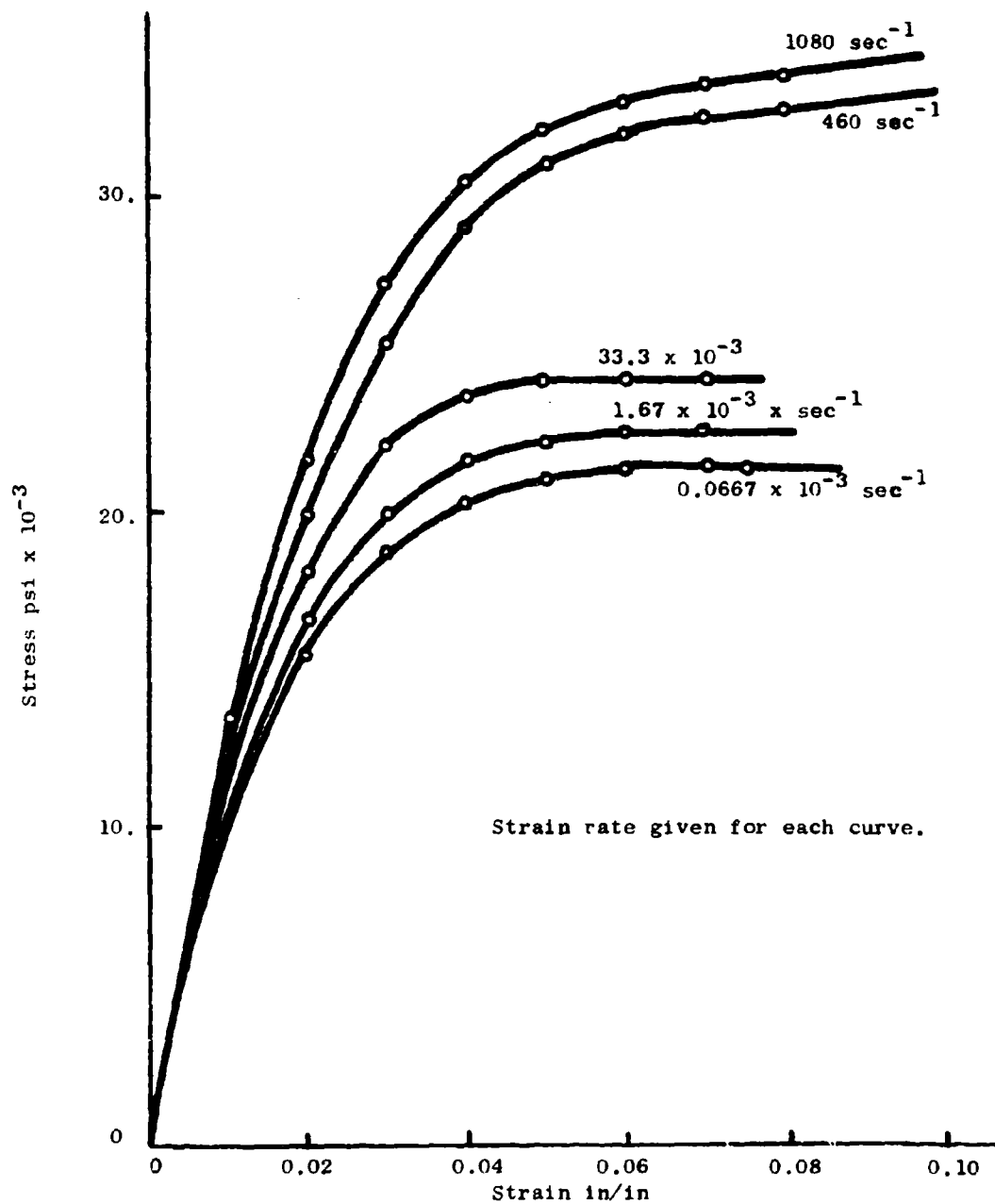


Figure 9. Stress-Strain Curves for Steel-Epoxy Composites
 $V_f = 10\%$ Wire Dia. = 0.004 in.

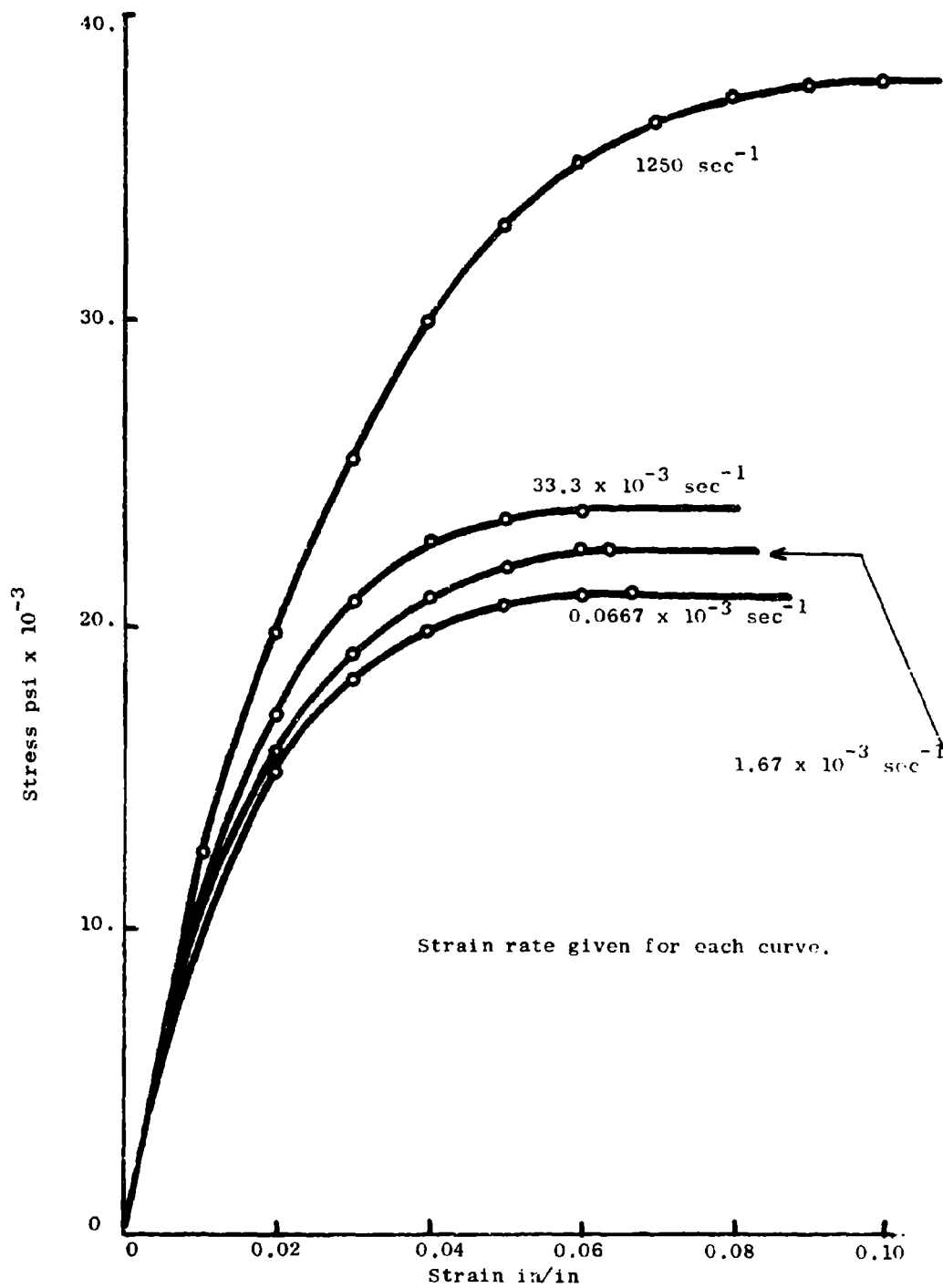


Figure 10. Stress-Strain Curves for Steel-Epoxy Composites
 $V_f = 10\%$ Wire Dia. = 0.008 in.

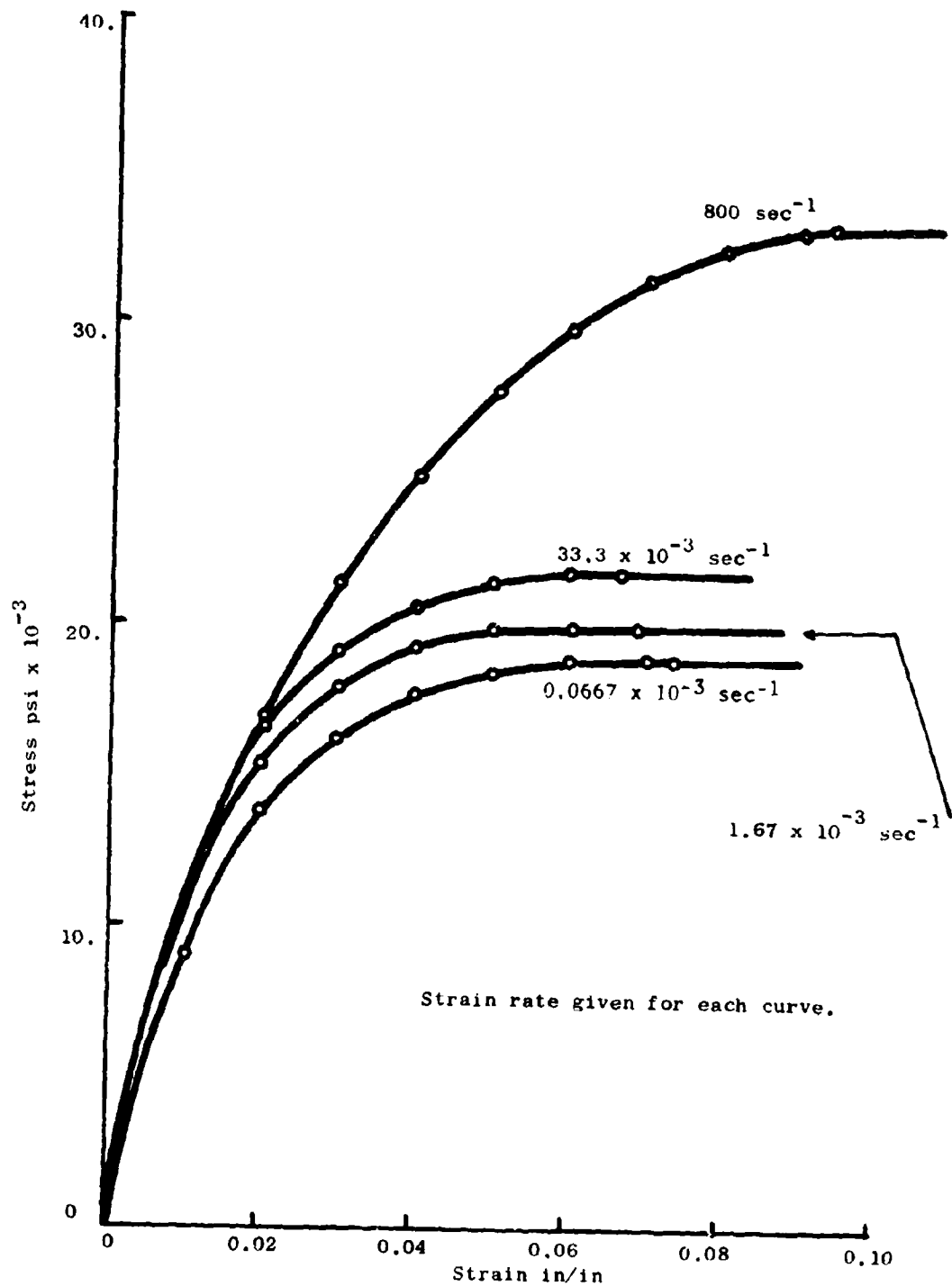


Figure 11. Stress-Strain Curves for Steel-Epoxy Composites
 $V_f = 10\%$ Wire Dia. = 0.016 in.

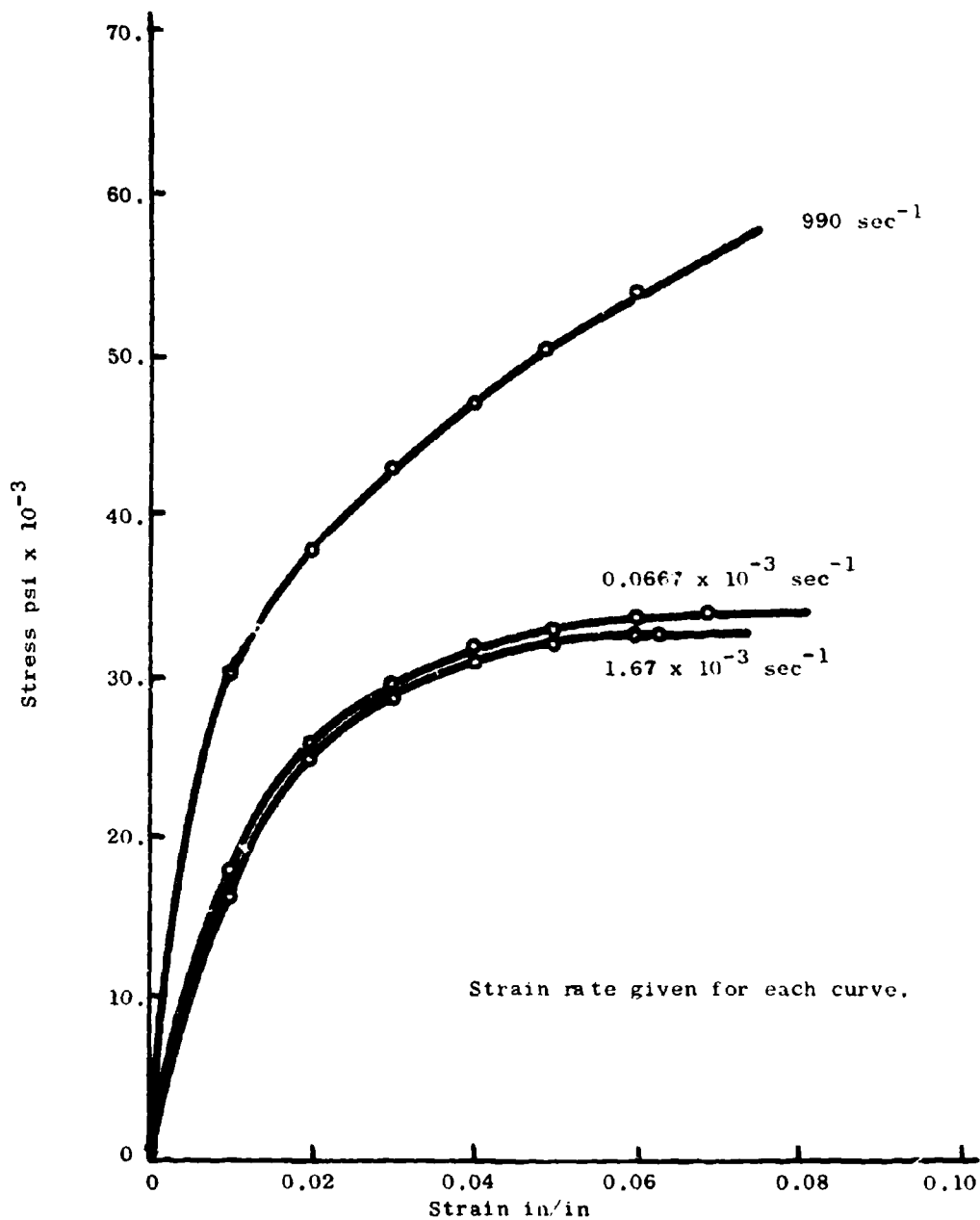


Figure 12. Stress-Strain Curves for Steel-Epoxy Composites
 $V_f = 26\%$ Wire Dia. = 0.008 in.

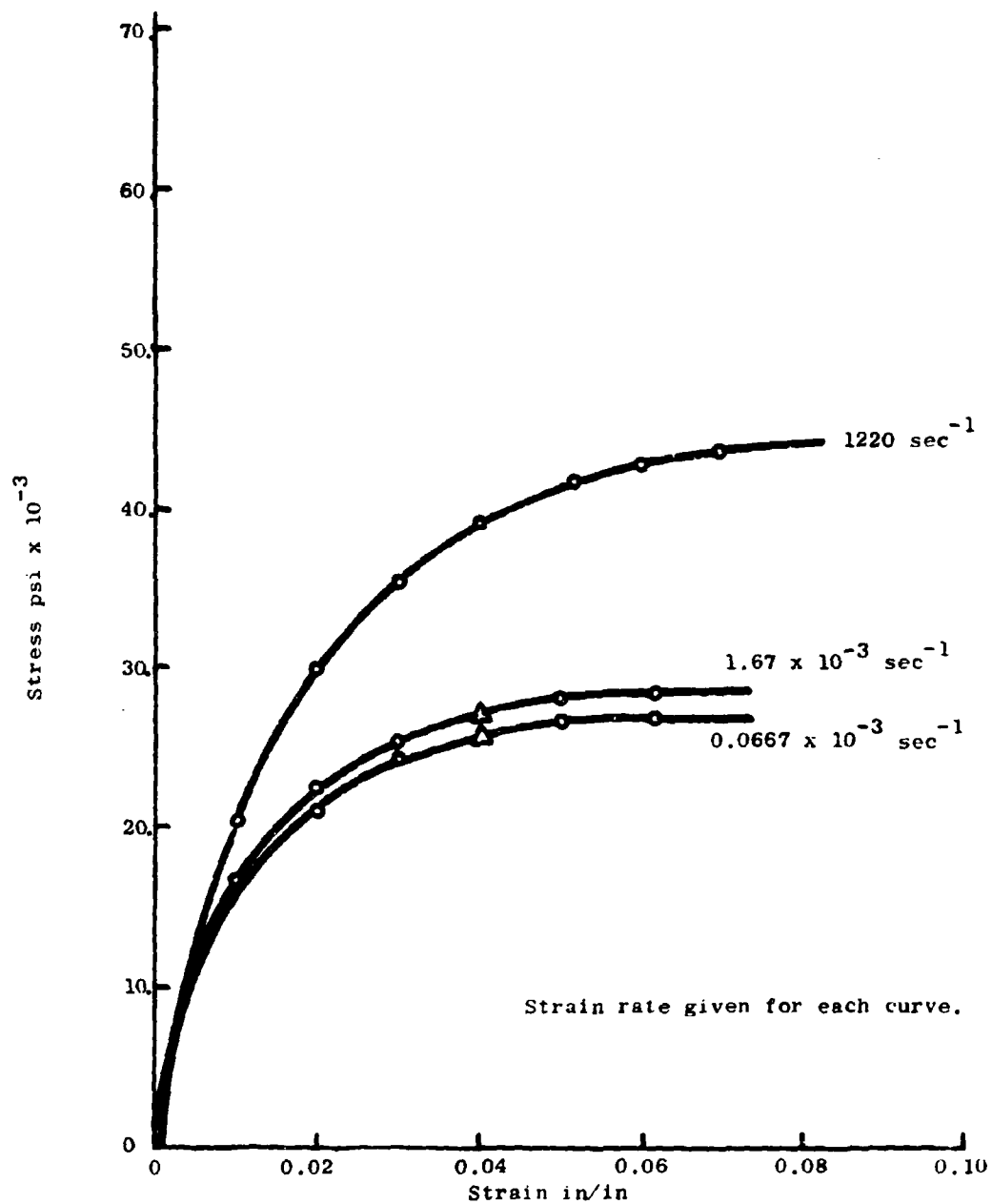


Figure 13. Stress-Strain Curves for Steel-Epoxy Composites
 $V_f = 26\%$ Wire Dia. = 0.016 in.

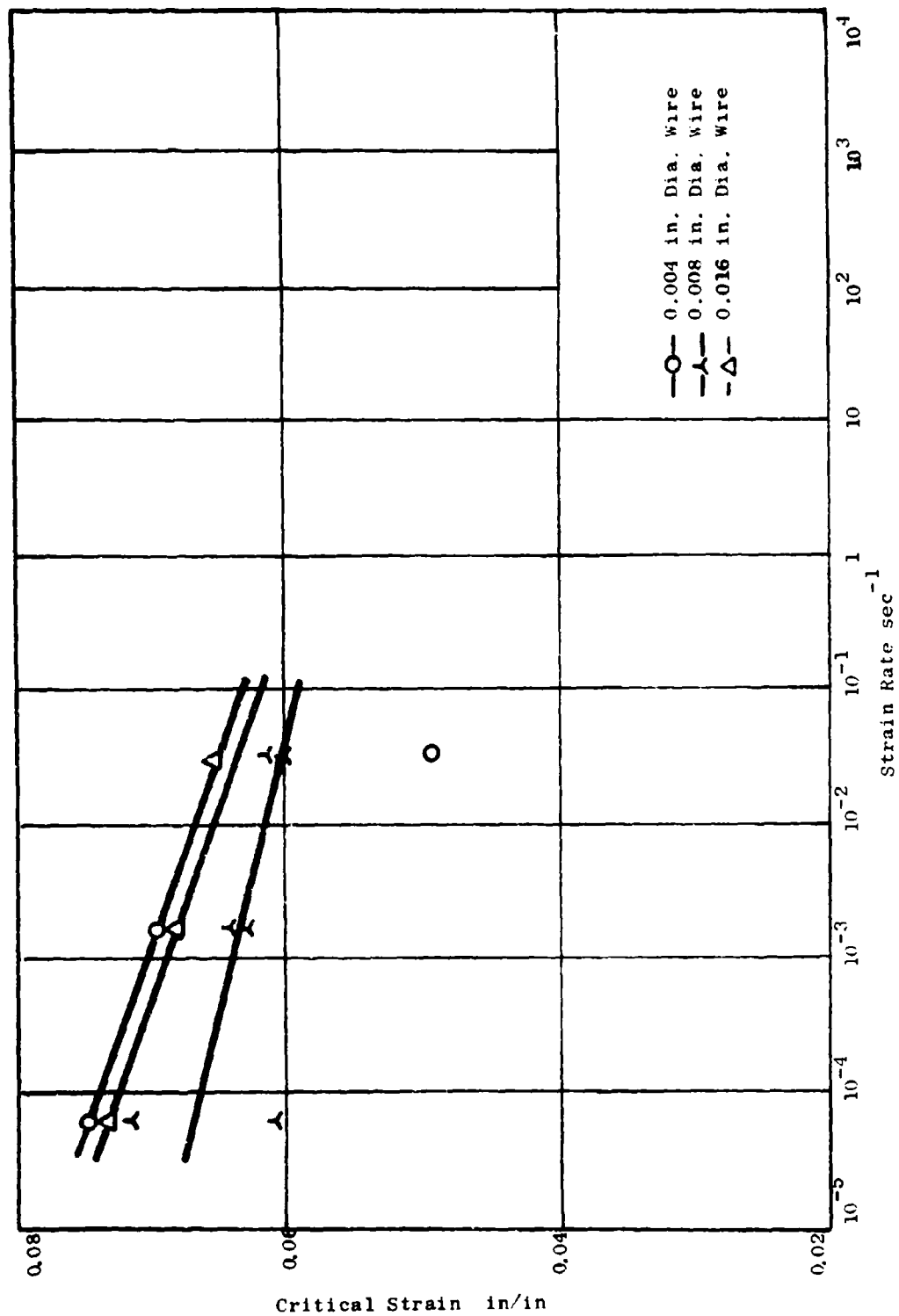


Figure 14. Critical Strain vs. Strain Rate For Steel-Epoxy Composites, $V_f = 10\%$

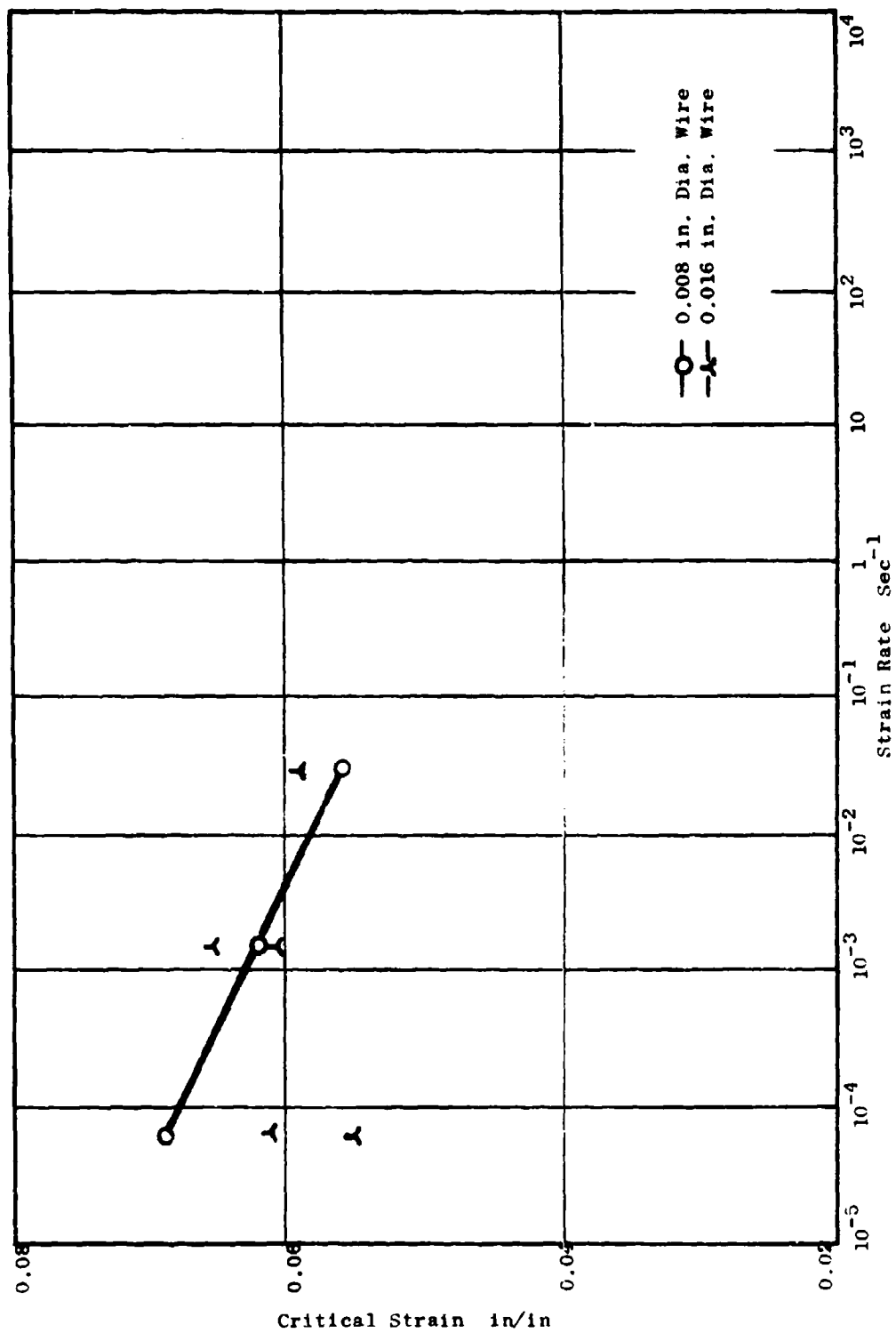


Figure 15. Critical Strain vs. Strain Rate For Steel-Epoxy Composites $V_f = 26\%$

selecting the strain at maximum stress, i.e. that corresponding to the horizontal tangent in the appropriate stress-strain diagram, and plotting the results. We note that for the case of steel-epoxy, 10% volume fraction, the material became more brittle with increasing strain rate. An exact trend in terms of the effect of wire size cannot be firmly identified, principally because of the judgment factor in selecting the amount of strain occurring at the maximum stress level. It would appear, however, that based on the present data there may be a reduction in the critical strain with increasing wire size.

In Figures 16 through 20 plots of stress versus strain rate with strain as a parameter are shown. These results indicate that at the lower strain rates there is a minimal effect of strain rate (low rate sensitivity) for the low volume percent materials. However, as we change to higher volume percents, there appears to be a change from positive to negative strain rate sensitivity. These effects are further demonstrated in Figure 21, which shows a comparative plot of maximum stress versus strain rate for varying wire sizes and volume percent of materials tested. It can be seen that for an 8 mil diameter wire in a 26% volume fraction composite we have a negative dependency on strain rate. Further, as we increase the wire size and volume percent of reinforcing material we find that a transition region develops which emphasizes a change in strain rate sensitivity as a function of stress level. This is readily seen once again in Figure 21, which summarizes much of the data presented in Figures 16 through 20 and which show a comparison with the basic epoxy system.

In Figure 22, the distinct failure modes observed for the steel-epoxy specimens during testing at varying strain rates is documented. The figures indicate that the principal mode of failure is a shear type failure associated with fiber buckling. Another type of microinstability failure mode has been observed, and is shown in Figure 22 for the 10% volume fraction, specimen with 0.016 inch wire diameter. The sinusoidal variation in wire appearance near the loaded end of the specimen is clearly evident. There appeared to be no appreciable difference in failure modes for those steel-epoxy specimens tested which had fiber end faults (Figures 3 through 5). Indeed, failure appeared to be insensitive to the inherent material faults present.

Representative dynamic stress-strain curves, as obtained from Hopkinson Pressure Bar Tests for the steel-epoxy specimens as shown in Figure 23. Included for comparative purposes is data on a pure epoxy specimen. Specific values of stress and strain levels have not been shown since these require appropriate

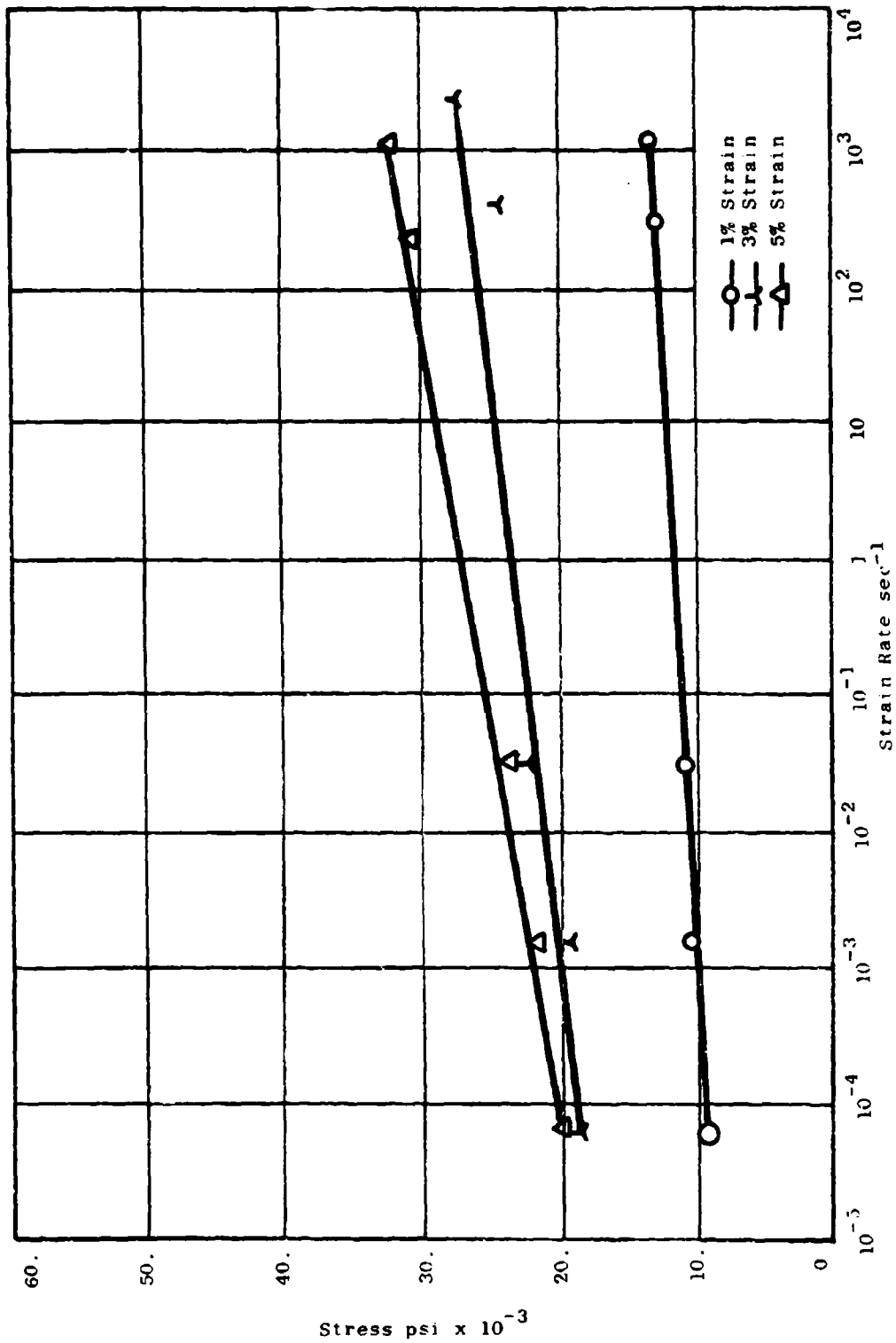


Figure 16. Stress vs. Strain Rate For Steel-Epoxy Composites $V_f = 10\%$, 0.004 in.

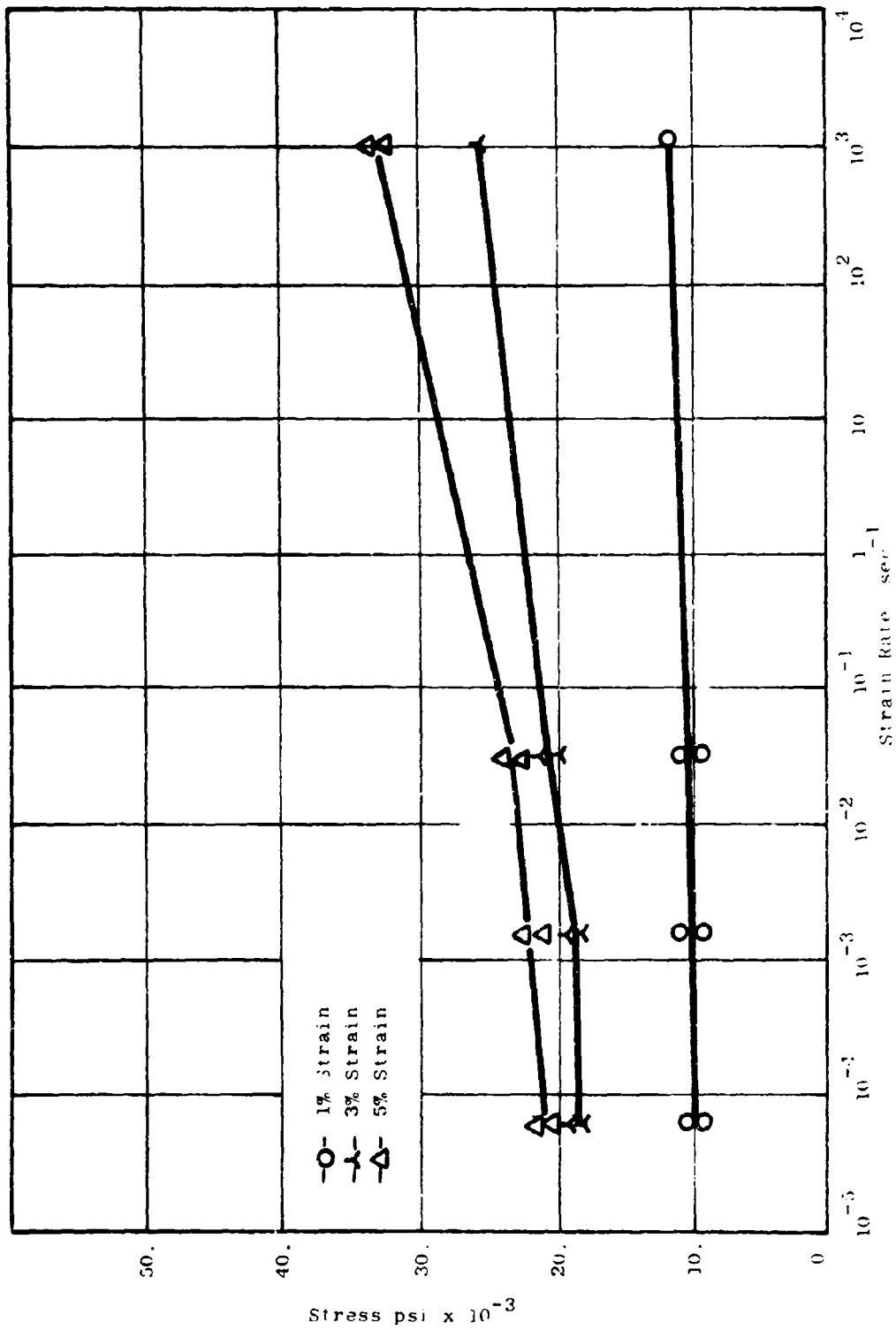


Figure 17. Stress vs. Strain Rate With Varying Strain Steel-Epoxy Composites $\epsilon_f = 10\%$, 0.008 in. Wire Dia

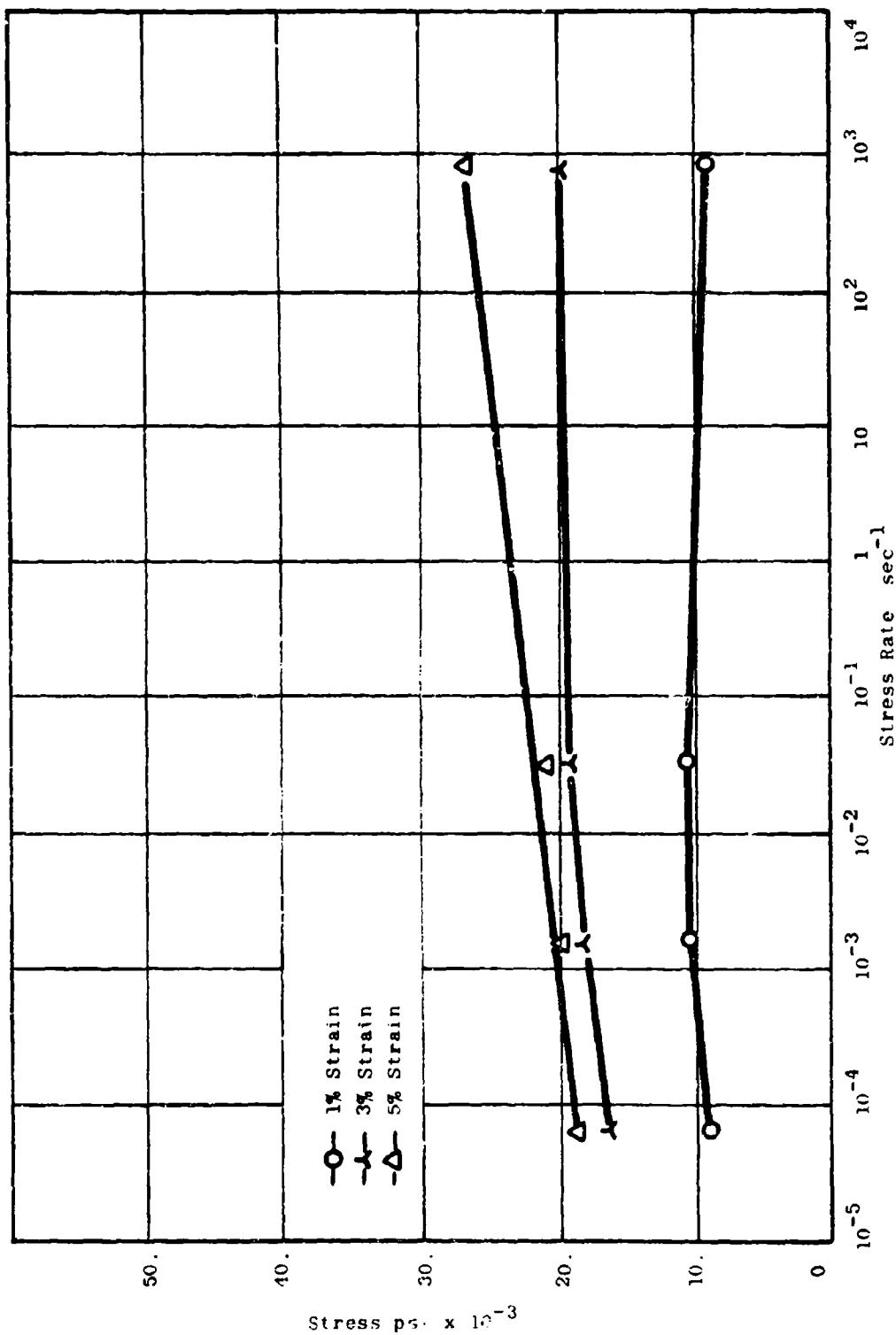


Figure 18. Stress vs. Strain Rate with Varying Strain Steel-Epoxy Composites
 $V_f = 10\%$, Wire Dia. = 0.016 in.

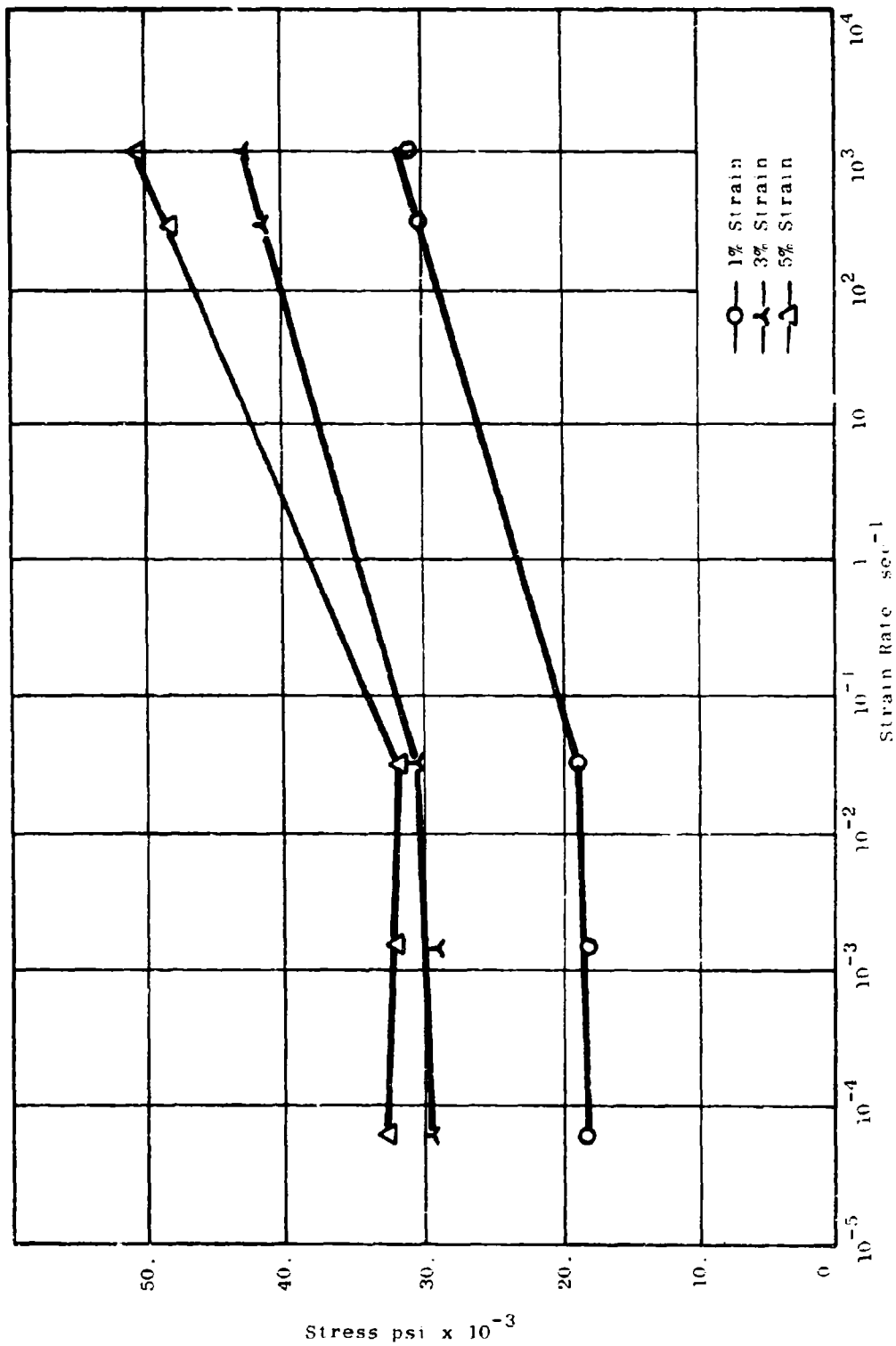


Figure 19. Stress vs. Strain Rate with Varying Strain Steel-Epoxy Composites
 $V_f = 26\%$, Wire Dia. = 0.008 in.

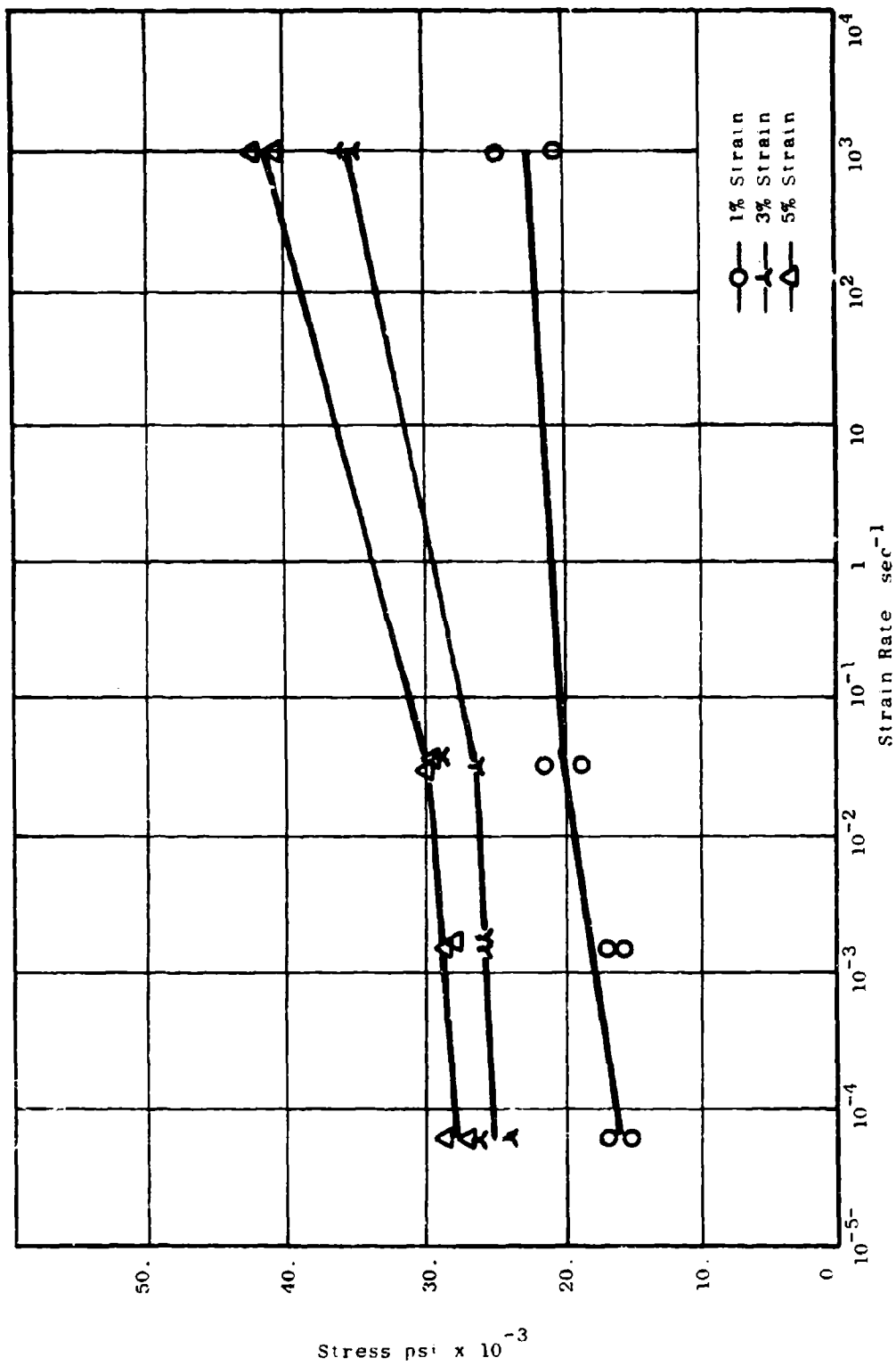


Figure 20. Stress vs. Strain Rate with Varying Strain Steel-Epoxy Composites
 $V_f = 26\%$, Wire Dia. = 0.016 in.

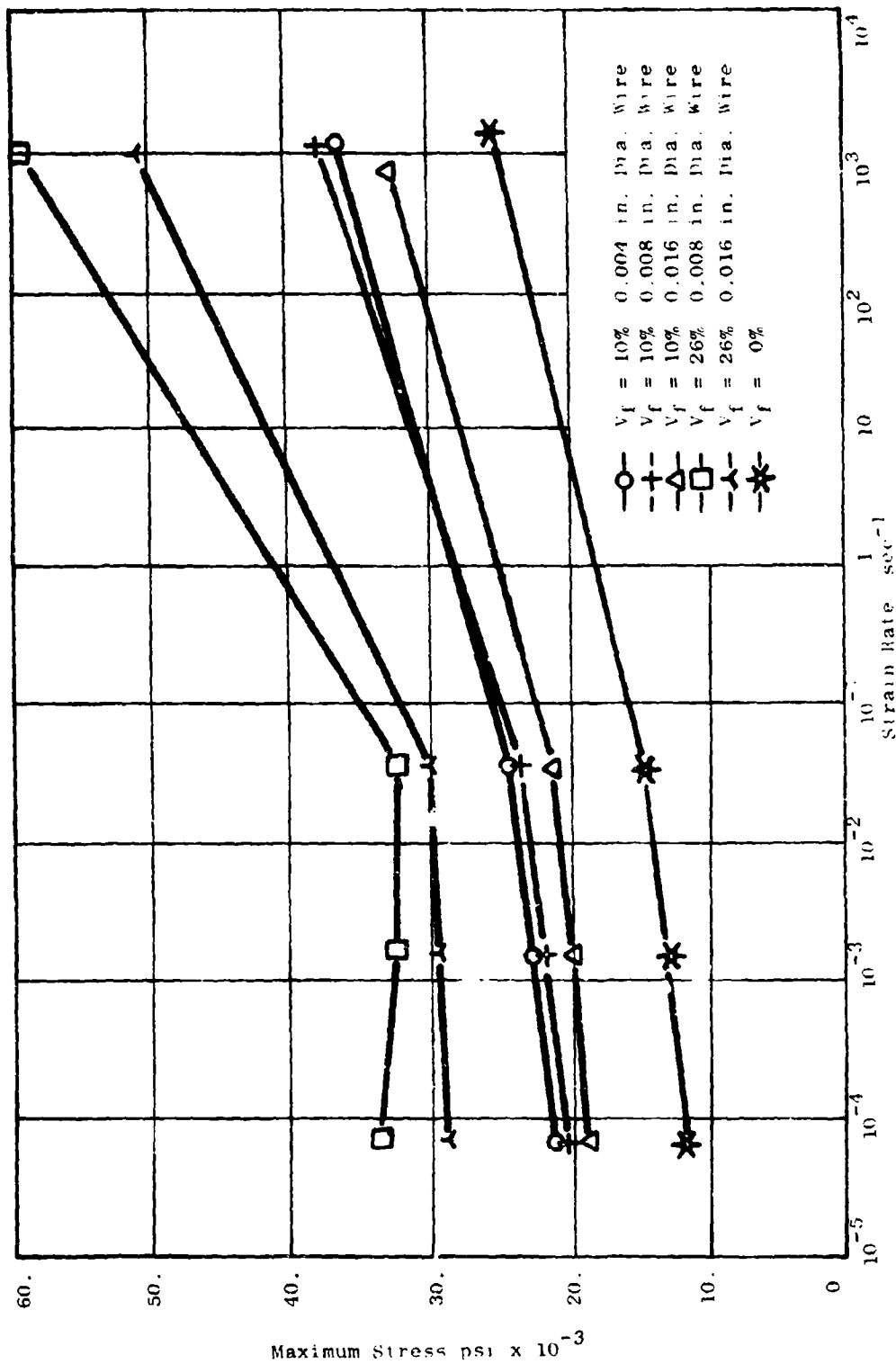


Figure 21. Maximum Stress vs. Strain Rate for Steel-Epoxy Composites

STEEL EPOXY COMPOSITES
FAILURE MODES

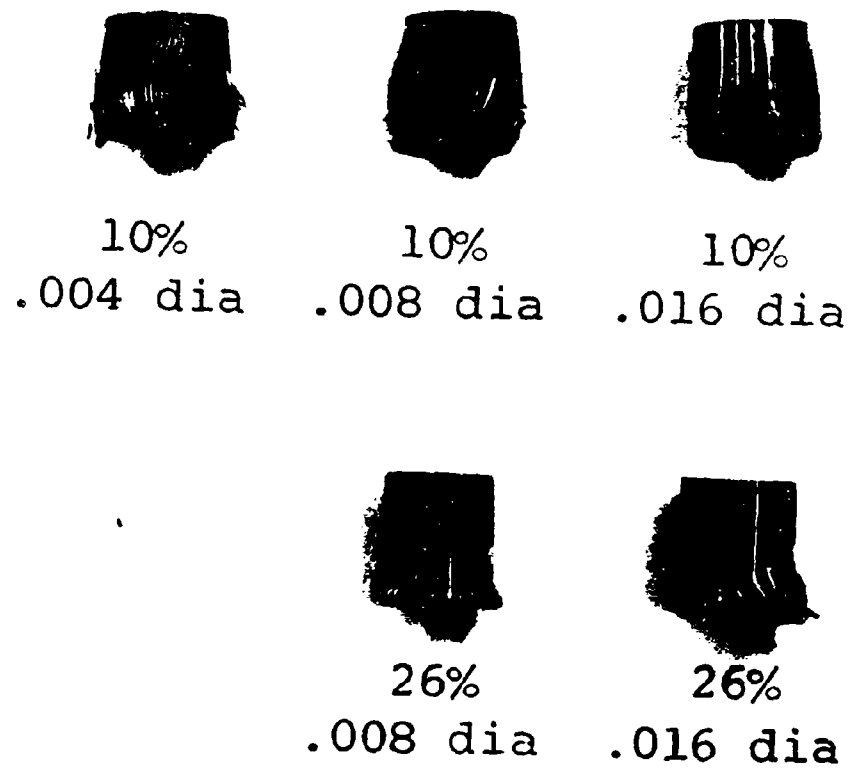
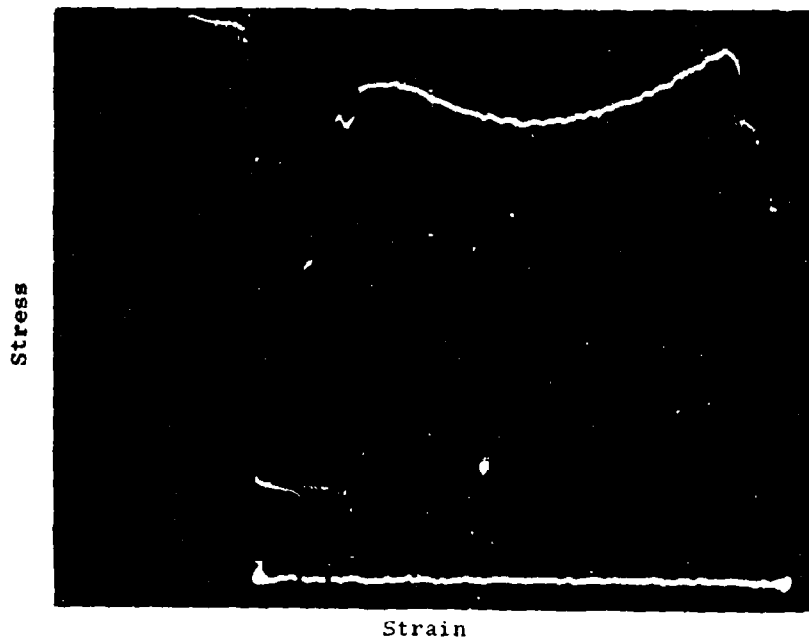
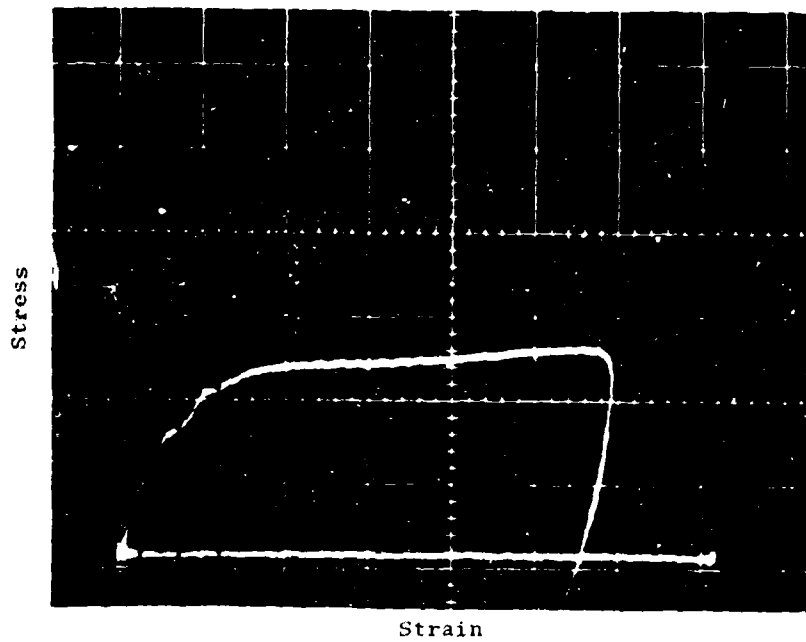


Figure 22. Steel-Epoxy Composites, Failure Modes

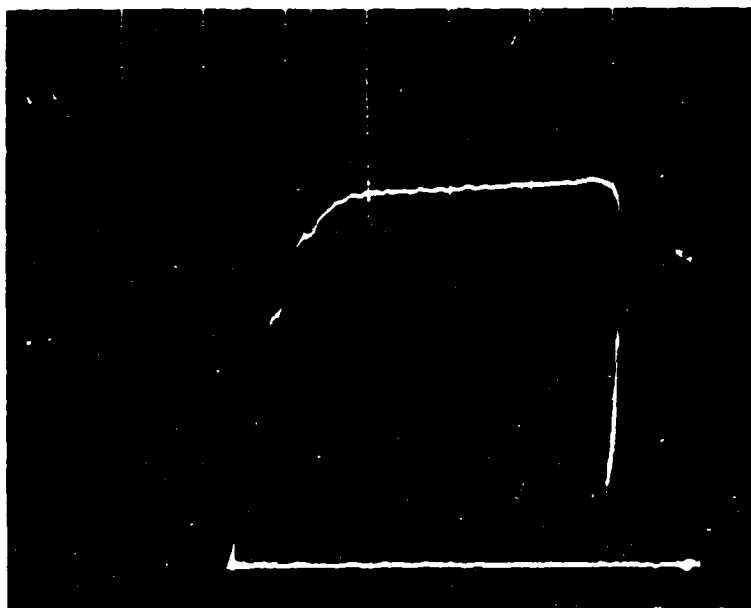


(a) Epoxy $V_f = 0\%$



(b) $V_f = 10\%$, Wire Dia. = 0.004 in.
Figure 23. Dynamic Stress-Strain Curves

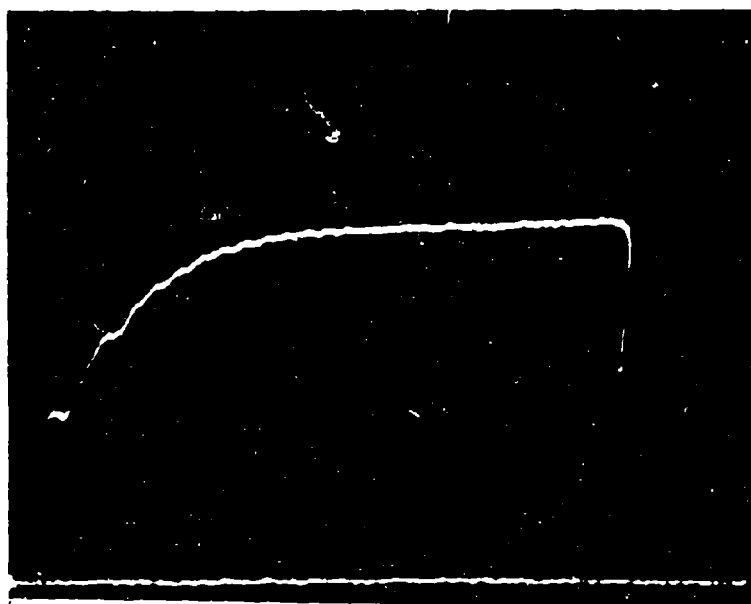
Stress



Strain

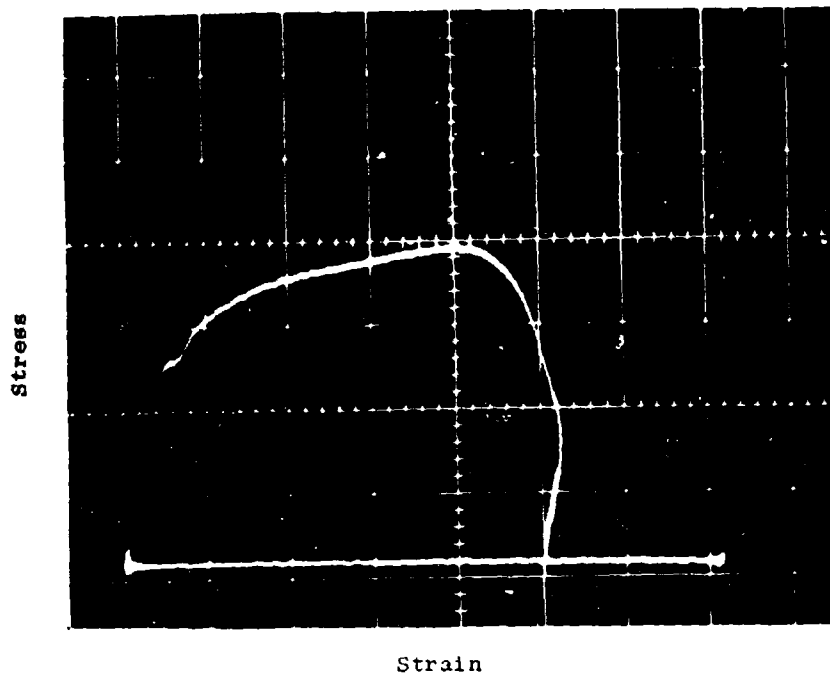
(c) $V_f = 10\%$, Wire Dia. = 0.008

Stress

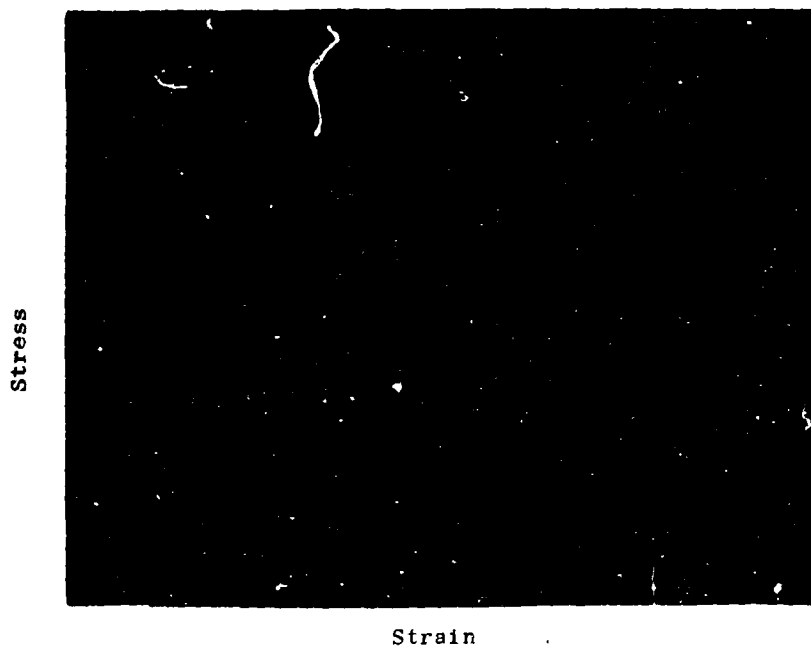


Strain

(d) $V_f = 10\%$, Wire Dia. = 0.016 in.
Figure 23. Dynamic Stress-Strain Curves



(e) $V_f \approx 26\%$, Wire Dia. = 0.008 in.



(f) $V_f \approx 26\%$, Wire Dia. = 0.016 in.

Figure 23. Dynamic Stress-Strain Curves

calibration factors. The curves, however, display qualitatively the nature of the observed dynamic stress-strain diagrams as a function of wire size and volume percent wire reinforcement.

4.1.2 Fiberglass

As a representative composite system of the inorganic matrix type, reinforced by continuous inorganic filaments, a fiberglass system was evaluated. The particular system obtained had a volume percent of reinforcing filament of 61% fiberglass, with fiber diameter of approximately 0.000037 inches. These samples, as previously mentioned, were obtained from commercial sources. As in the preceding case, plots of stress versus strain, critical strain versus strain rate, maximum stress versus strain rate, and stress versus strain rate for varying levels of strain are shown in Figures 24 through 27. For fiberglass specimens, it is apparent that there is considerable strain rate sensitivity at the lower levels of strain rate, with a reduction in this sensitivity occurring with increasing strain rate. In addition, as in the case of the steel reinforced epoxy, we see from Figure 25 that the critical strain diminishes with increasing strain rate. This is to be expected as the material becomes embrittled with increasing strain rate. In Figure 26 we note the increase in stress with a strain rate for varying levels of strain. For this particular system it is noted that there is considerable variation in the strength levels at the corresponding strain levels as tested. This is due to the steep slope of the stress-strain curves and the resulting sensitivity of the stress to the exact strain value used. In general, the static and dynamic curves had the same shape and failure resulted in a sudden and drastic reduction of load carried by the specimen at a maximum strain of approximately 2% in all samples tested.

The failure modes of the fiberglass specimens are documented in Figure 28 for the various strain rates tested. The brittle nature of the fracture behavior, accompanied by large segmented fragments is evident.

A typical dynamic stress-strain curve, as obtained in a Hopkinson Pressure Bar test, is shown in Figure 29. Again, specific values of stress-strain levels have been omitted. The brittle nature of these composites is evident, with almost complete unloading occurring after the maximum stress has been obtained. The low strain rate, stress-strain results were quite similar.

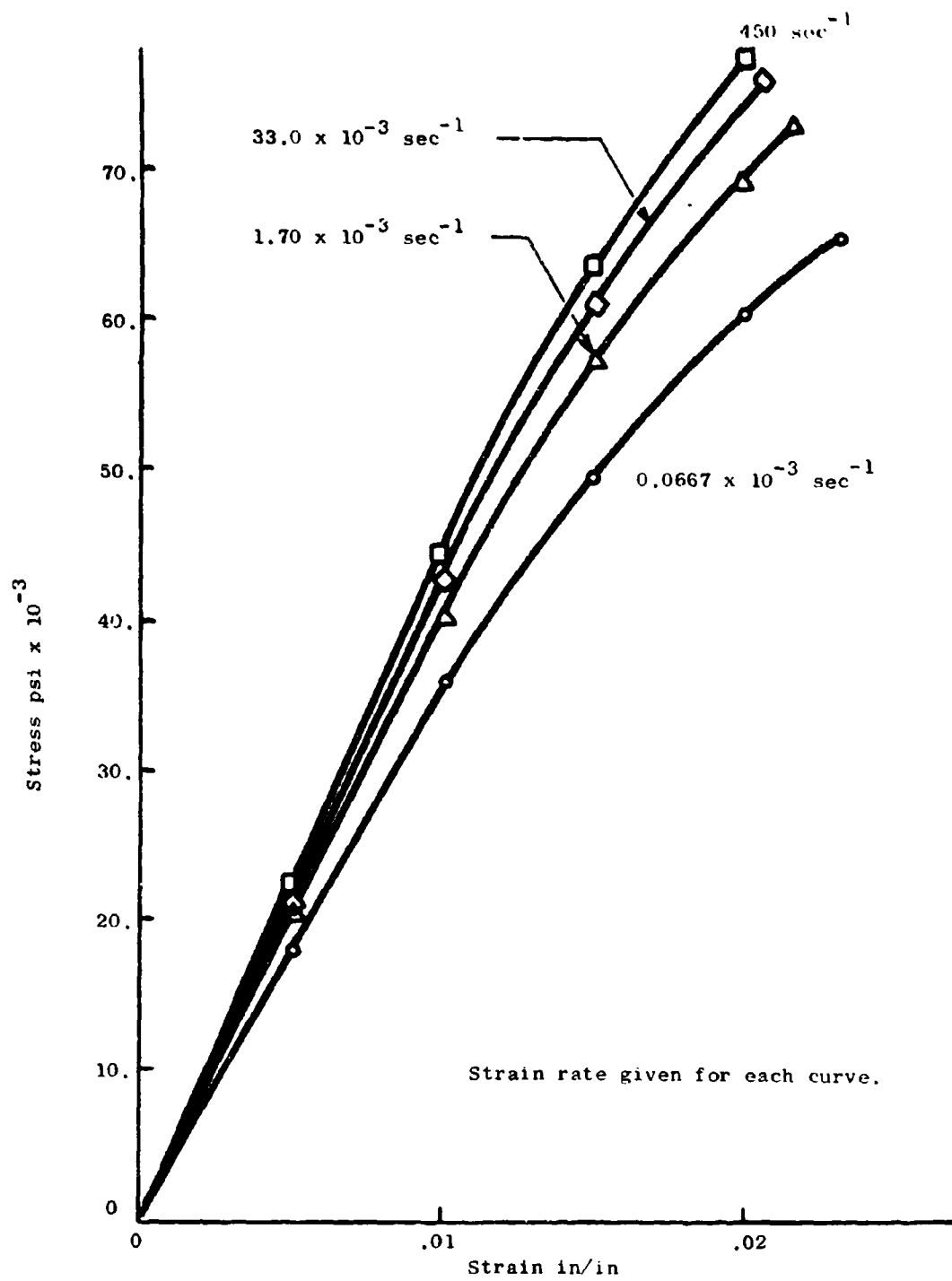


Figure 24. Stress-Strain Curves, Fiberglass Composite

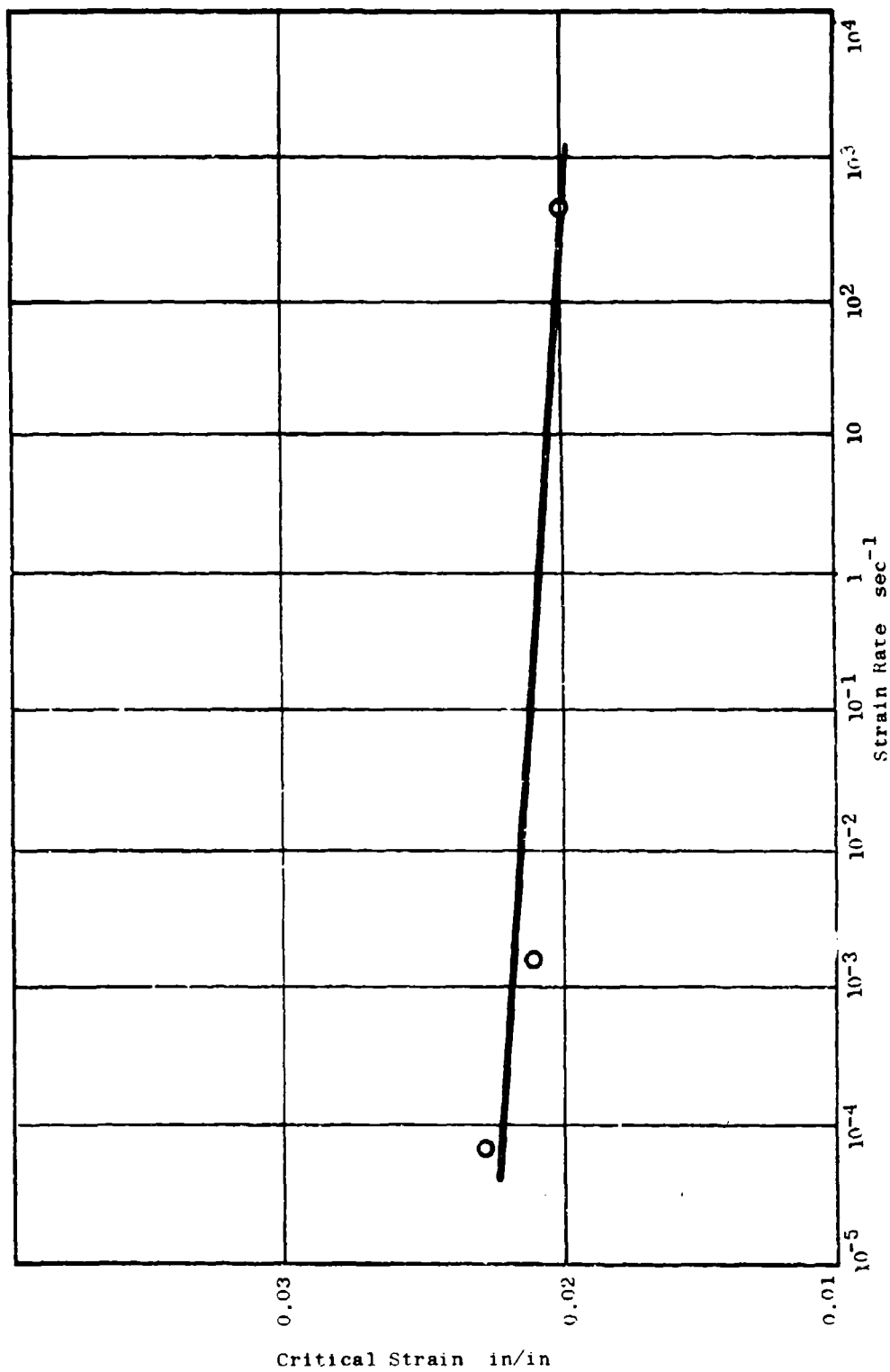


Figure 25. Critical Strain vs Strain Rate, Fiberglass Composite

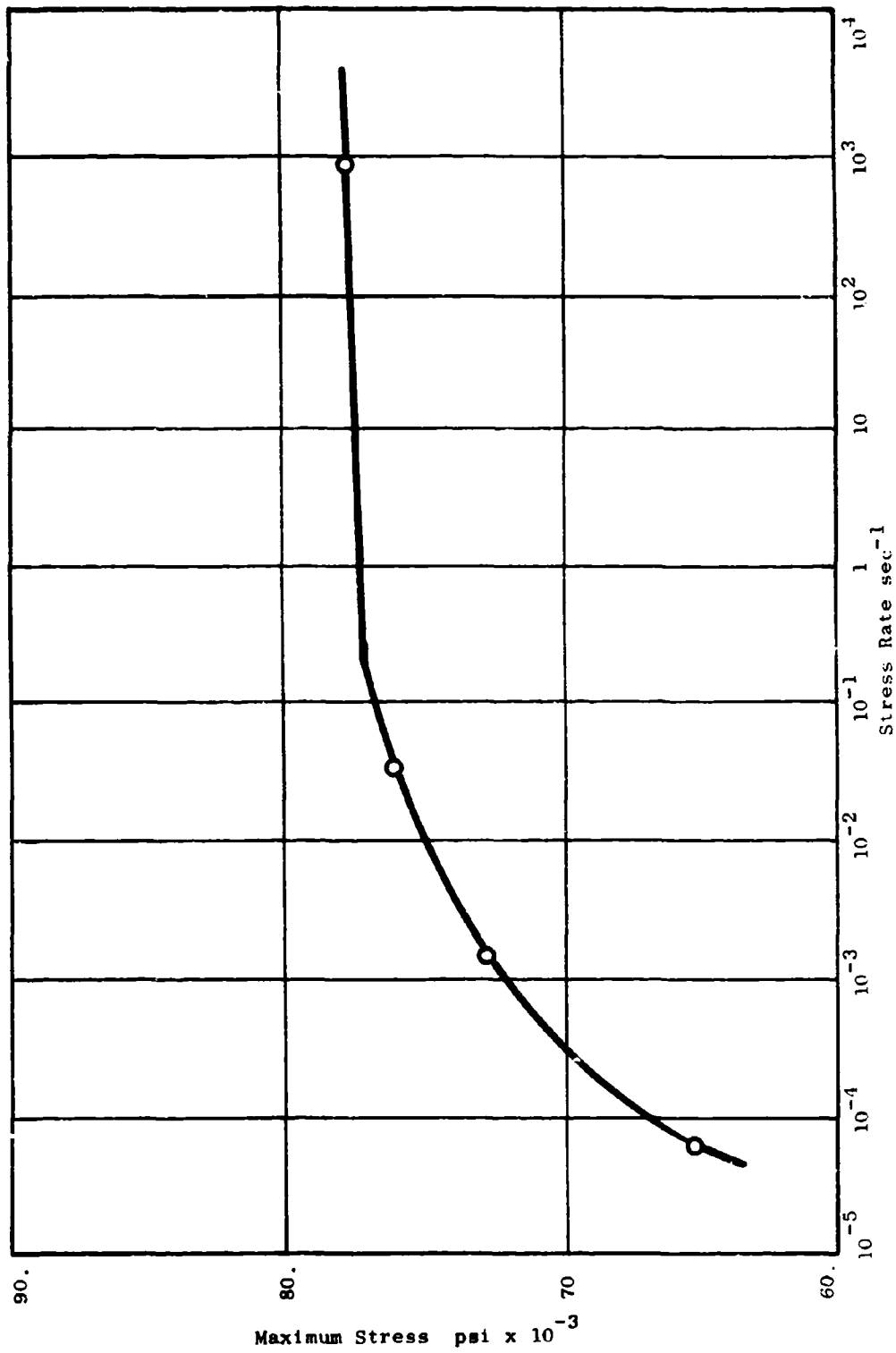


Figure 26. Maximum Stress vs. Strain Rate. Fiberglass Composite

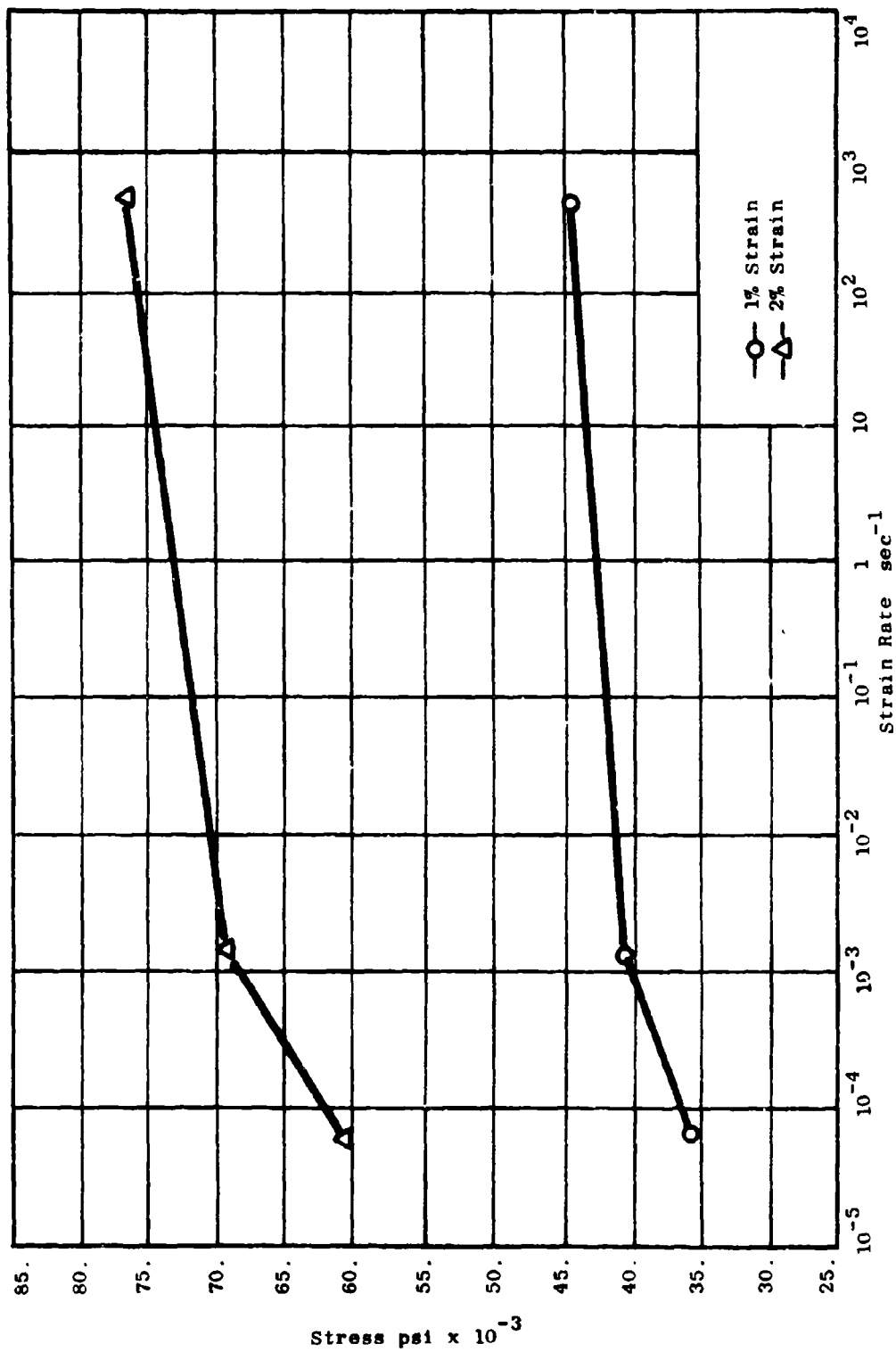


Figure 27. Stress vs. Strain Rate with Varying Strain, Fiberglass Composite

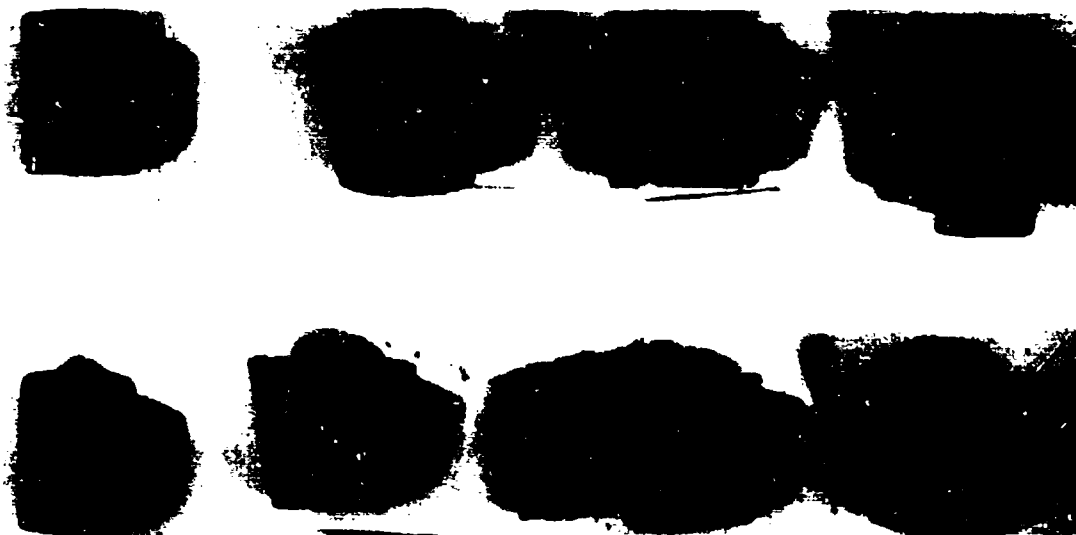


Figure 28. Fiberglass Composites, Failure Modes

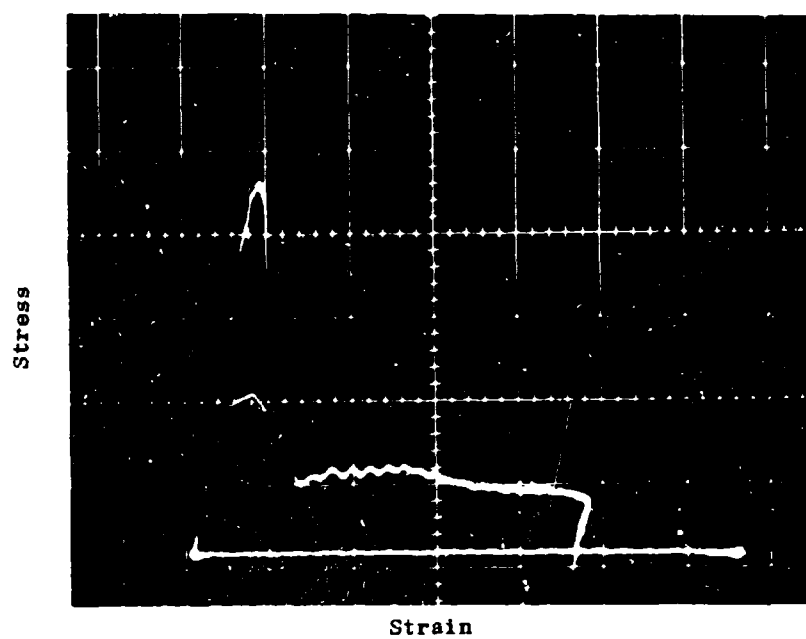


Figure 29. Dynamic Stress-Strain Curve for Fiberglass Composite

4.1.3 Aluminum-Nickel (Al-Al₃Ni)

Results for a 'discontinuous' (the meaning of 'discontinuous' for Al-Al₃Ni eutectic systems is discussed in 127) inorganic reinforced inorganic matrix composite, represented by the aluminum-nickel samples, are shown in Figures 30 and 31. Each of the test in this sequence was carried to failure and the terminal points on the stress-strain curve shown in Figure 30 represent the actual load reversal in the stress-strain diagram. It is noted that the stress increases with strain rate, as is expected from conventional predictions. However, the failure compressive strain at the low strain rates is approximately 33% less than the corresponding tensile strain as described in 7. This reduction in materials strength is believed to be due to fiber failure mechanisms operative in compression that are not important, in tension. However, it is noted that at the high strain rates the compressive stress shows an increase of approximately 20% over typical low strain rate tensile test results. It is also observed from Figure 29 that the material loses its limited ductility with increasing strain rate, becoming almost linearly elastic to failure at the high strain rates.

Figure 30 shows stress versus strain rate curves at various strain levels. There appears to be a change in the strain rate sensitivity at intermediate strain rates; however, presently available test equipment did not allow representative data points to be obtained in this region, and thus the precise nature of the rate dependency could not be established.

The microstructure of the aluminum-nickel system consists of a series of plate-like and rod-like reinforcing elements of approximately micron size. The exact nature of the reinforcements is a function of the solidification rate. Tests of several substructures produced by varying solidification rates are planned for the next program phase. A typical dynamic stress-strain curve obtained from the Hopkinson Pressure Bar is shown in Figure 32.

4.2 Failure Dynamic Properties

In order to obtain information of the failure characteristics of the various composites tested in dynamic compression, an air gun, described in Section III was used. Several important specimen failure characteristics, particularly critical projectile velocity and qualitative fracture behavior of composites based on visual records, were sought.

In contrast to conventional monolithic materials, the compressive failure behavior of composites, as indicated in the

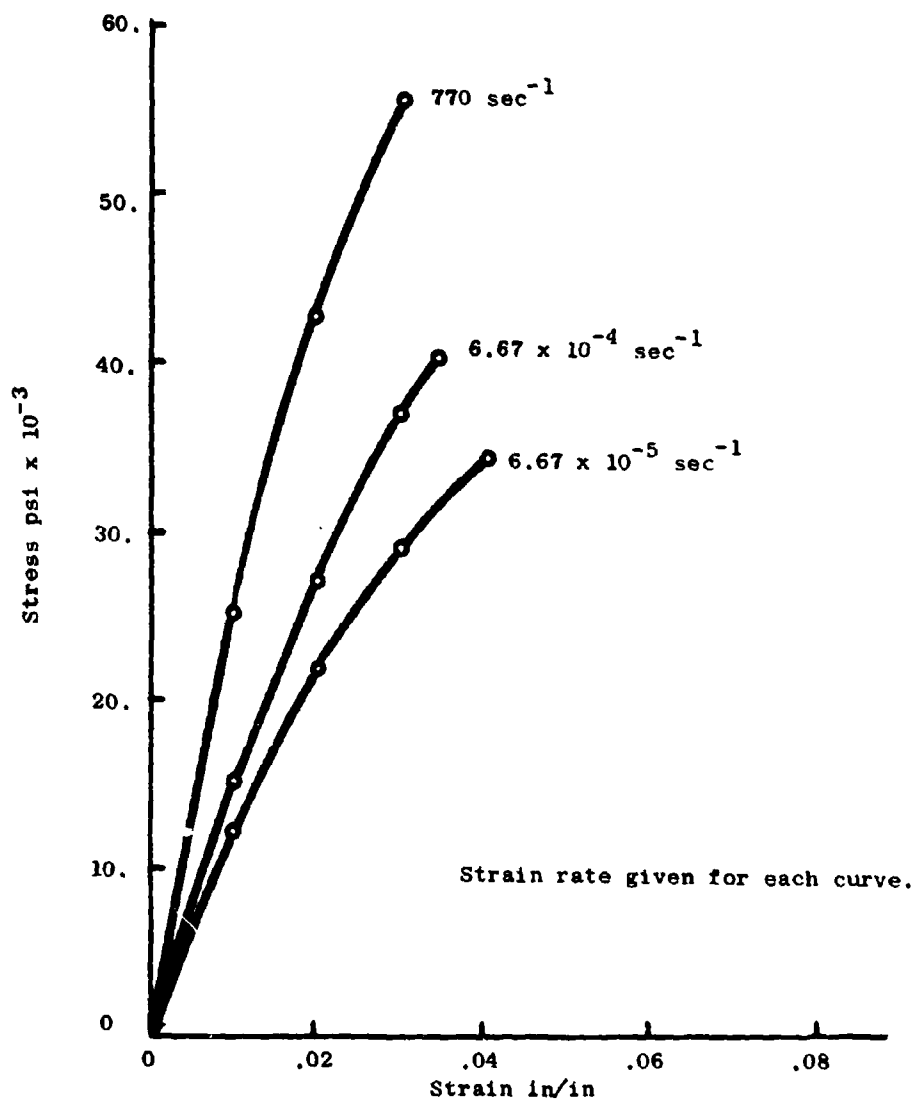


Figure 30. Stress-Strain for Aluminum Nickel Composite

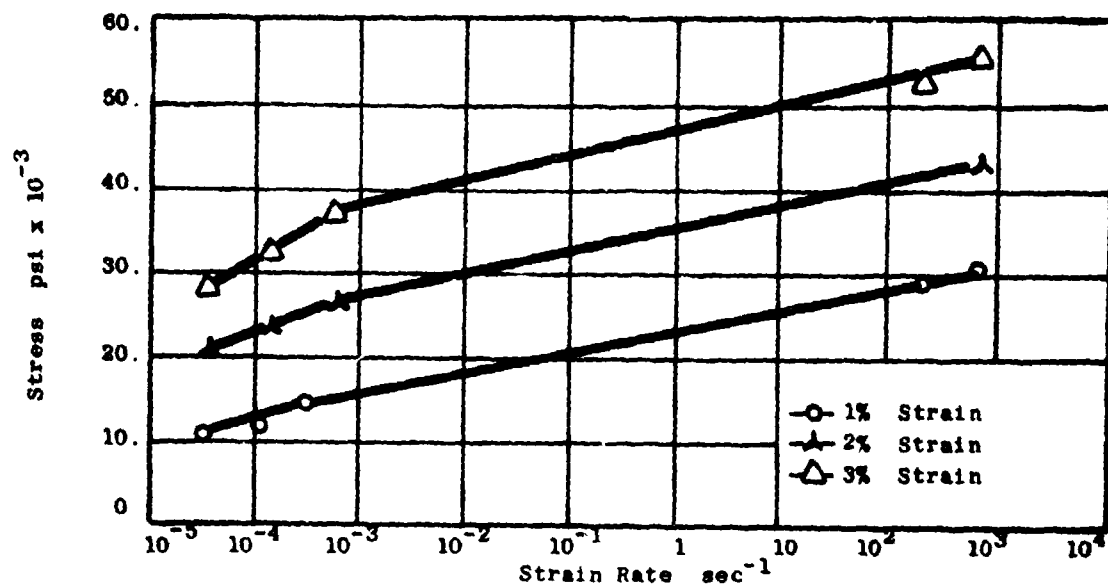


Figure 31. Stress vs. Strain Rate with Varying Strain, Aluminum-Nickel Composite

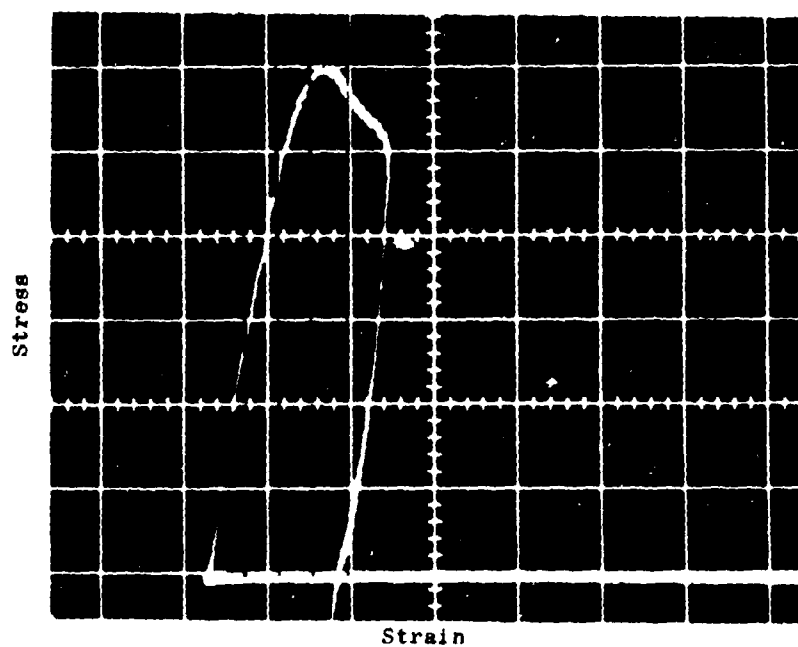


Figure 32. Dynamic Stress-Strain curve for Aluminum-Nickel Composite

technical background section, may be varied and complicated. For the steel epoxy composites, two distinct types of failure were observed. The first type of failure was associated with instability of the reinforcing wires. This is characterized by permanent bending or buckling of individual filaments and occurs at the point on the stress-strain curve where maximum stress is first attained (horizontal tangent). The second distinct failure type is complete fracture and fragmentation of the projectile. For this case, any amount of fragmentation was considered sufficient to define failure with the exception of failure occurring along a plane containing an obvious fault, or fragmentation due to asymmetrical impact caused by tumbling of the projectile.

One objective of the present test program was to attempt to correlate and predict, by some appropriate calculation, a relation between the high strain rate data obtained from the Hopkinson Pressure Bar tests and the actual failure dynamic studies carried out using the air gun assembly. In order to do this, several theoretical approaches were examined for their suitability for making such predictions. One approach was based upon the calculation of a critical velocity in compression for the specimens. This was based on the momentum principle of Von Karman [98] developed originally to predict critical velocities in tension from dynamic stress-strain data. It was possible to utilize this approach, based on the specific deformation characteristics at the high strain rates, for several of the composites studied in the present investigation. Based on this momentum approach, calculations were made and results obtained which predicted a critical velocity in the range of 3,000-4,000 in/sec. However, one of the primary difficulties in interpreting this result was a specific characterization of the type of failure which would occur at this particular velocity. Specifically, because of the complicated nature of the failure of composites, it was difficult to select an appropriate criterion for defining failure. Therefore, in the present investigation failure, as previously defined, was used for calculating critical velocities.

Considering these definitions, a simple approach based on equating impact energies to specimen energy absorption capability, as determined from the dynamic stress-strain data obtained by using the Hopkinson Pressure Bar was made. A tabulation of this data for steel-epoxy composites is shown in Table III. In addition, Figures 33 and 34 show plots of the critical velocity versus wire diameter for two volume percents of the steel epoxy series of specimens. The solid curves represent calculated predictions while actual test results are shown as data points for the various specimens. It is noted that two curves are shown, one for the critical velocity (V_p) and one for (V_f) as previously defined.

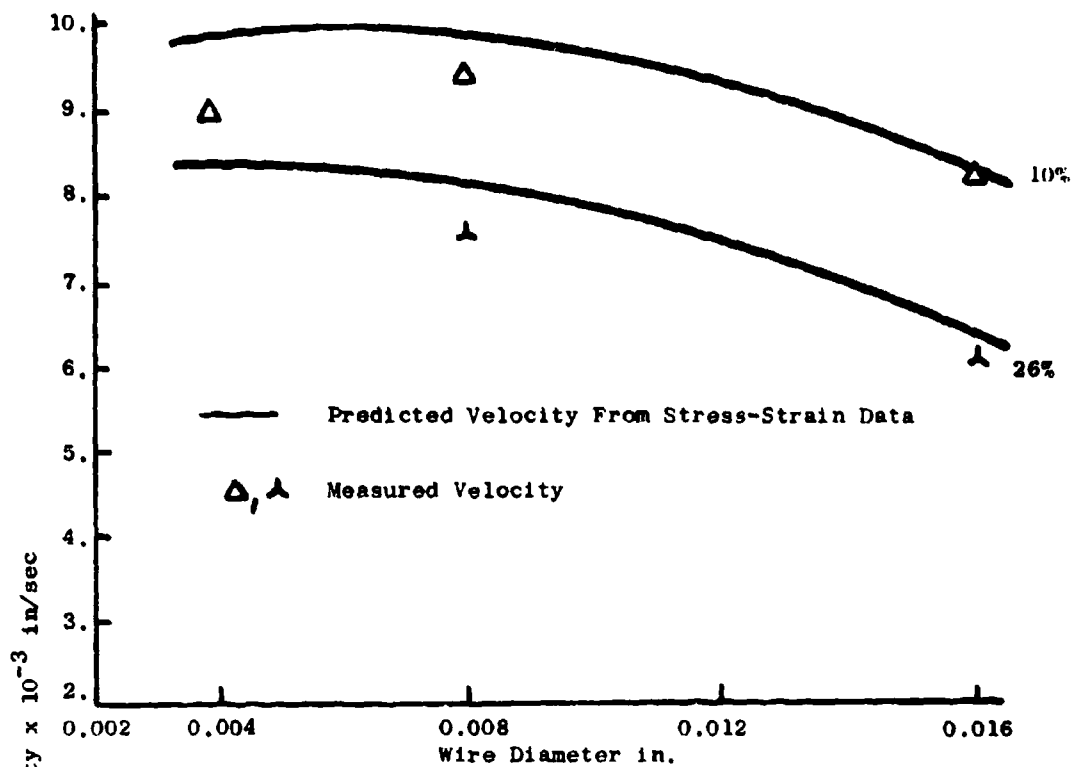


Figure 33. Critical Fracture Velocity vs. Wire Diameter for Steel Epoxy Composites $V_f = 10\%, 26\%$

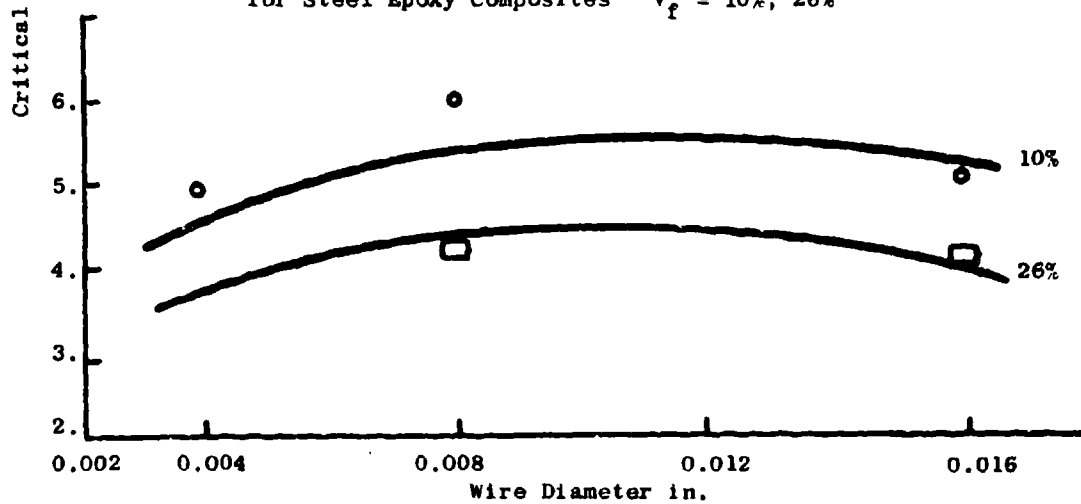


Figure 34. Critical Plastic Flow Velocity vs. Wire Diameter for Steel Epoxy Composites $V_f = 10\%, 26\%$

TABLE III. CRITICAL VELOCITIES FOR STEEL-EPOXY COMPOSITES

Composite	$(V_p)_c$ (in/sec)		$(V_f)_c$ (in/sec)	
	calc.	meas.	calc.	meas.
10% - .004 dia	4500	5000	9880	9000**
10% - .008 dia	5350	6000*	9860	9050**
1% - .016 dia	5120	5000	8280	~ 8250
26% - .008 dia	4350	3800	8100	7500
26% - .016 dia	3890	4000	6300	6000**

*Lowest Velocity Tested

**Highest Velocity Tested

The critical velocity labeled $(V_p)_c$ was calculated by equating the projectile kinetic energy to that portion of the Hopkinson Pressure Bar stress-strain diagram for which a horizontal line through the maximum stress level, or average stress level, could be determined. The complementary critical velocity $(V_f)_c$ relating to composite separation or delamination, was calculated by equating projectile kinetic energy to the total area under the Hopkinson Pressure Bar stress-strain diagram to failure. It should be noted that the strain rates in the gas gun experiments were approximately one order of magnitude greater than the corresponding Hopkinson Pressure Bar Data, that is $\dot{\epsilon}_{\text{air gun}} \sim \times 10^4$ in/in/sec. However, the area under the curve is sufficiently insensitive to strain rate that the pressure bar results were used without correction.

From these data we observe an extremely good correlation between predictions and test results for early specimen failure and ultimate specimen fracture. In both cases there appears to be an optimum wire size for a particular volume percent reinforcement which will generally yield an optimum critical velocity. Further documentation of these results is shown in Figures 35 and 36 which show the specific specimens tested for which comparisons were made and the deformation characteristics obtained.

For all the specimens which were tested by the air gun assembly, a high speed photographic series of the mushrooming failure characteristics plus post test photos were taken. These photo sequences were then used to determine the dynamic failure mechanisms and to compare these mechanisms with those observed in the quasi static and high strain rate pressure bar tests.

It was observed that for the steel reinforced epoxy specimens considerable heat was generated upon impact. The increase in

STEEL EPOXY COMPOSITES

10% Volume Fraction of 0.016 Dia. Wire
Velocity given in inches per second

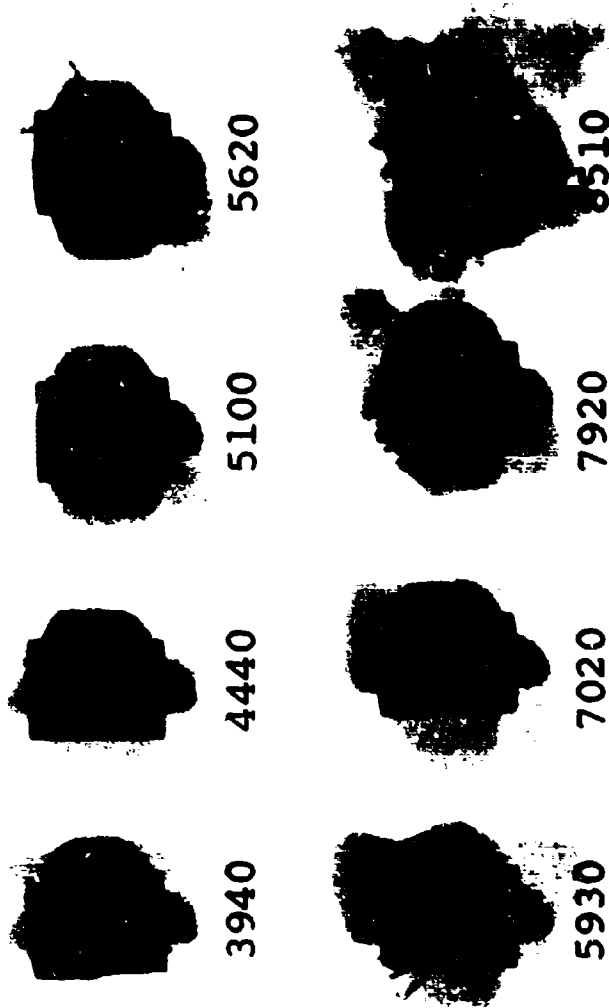


Figure 35. Dynamic Deformation at Various Impact Velocities Steel-Epoxy Composites $V_f = 10\%$ Wire Dia. $= 0.016$

STEEL EPOXY COMPOSITES

26% Volume Fraction of 0.016 Dia. Wire
velocity given in inches per second

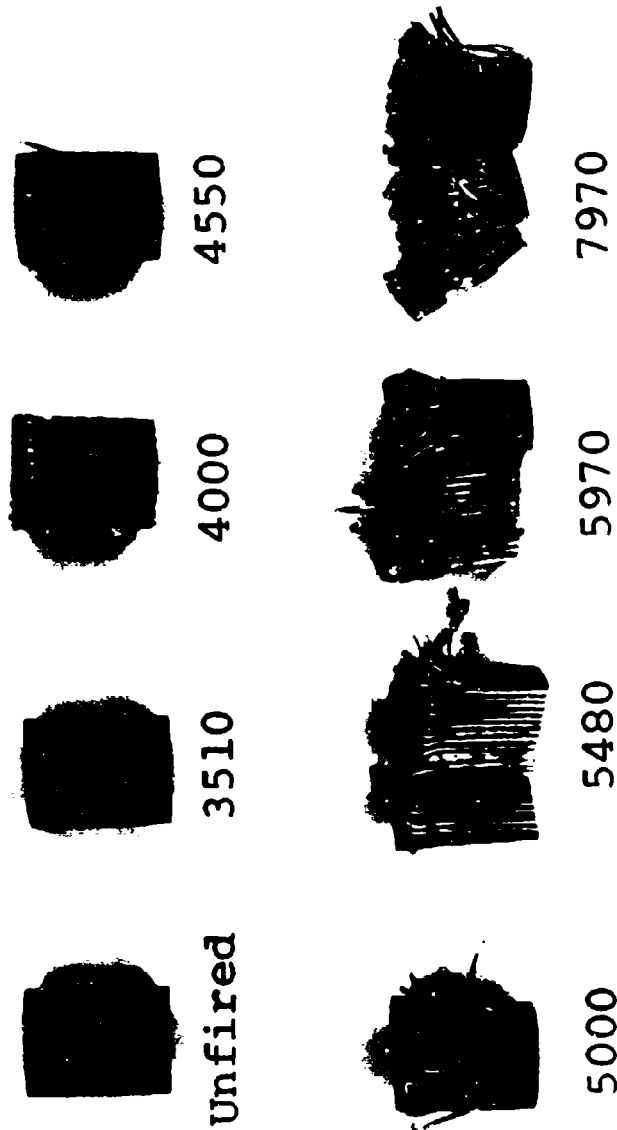


Figure 36. Dynamic Deformation at Various Impact Velocities Steel-Epoxy Composites
 $V_f = 26\%$ Wire Dia. = 0.016

temperature produced a reduction in strength of the epoxy matrix which allowed greater deformation of the specimens that would otherwise occur. However, when the specimen was removed from the firing range, it was noted that the specimen had relaxed to nearly its original shape while the fiber reinforcing elements remained in their buckled position. Also, the time in which the steel-epoxy specimens remained in contact with the target material was greater than for conventional monolithic materials. Photographs of the dynamic fracture behavior of these composites are shown in Figure 37. The failure modes observed in the gun tests appear to exhibit several features distinct from those observed in the Olsen and Pressure Bar tests. However, quantitative evaluation has been postponed until further data is obtained in the next phase of the program.

A limited number of aluminum-nickel projectiles were fired at a rigid target. A photographic display of the failure behavior of the aluminum-nickel material as compared with a 2024-T4 aluminum sample is shown in Figure 38. As can be seen, there is considerable local deformation near the impact face of nickel sample. This increased localization is attributed to the energy absorbing effects of the micron size reinforcing elements rotating and sliding through the matrix material in the local impact region. This interpretation seems confirmed by the lowest strain rate tests which showed a peculiar localized shear deformation near the end faces which occurs for such a reinforced system. Here also, the discontinuous reinforcing elements appear to slide and rotate with respect to one another in localized slip areas near the compressive loading regions.

For the fiberglass specimens, Figure 34 shows the brush-like failure occurring under impact of the composite specimens. This failure appears qualitatively similar to the behavior occurring in other testing procedure.

(a) $V_f = 10\%$
.004 Wire Dia.
8,970 in/sec

(b) $V_f = 10\%$
.008 Wire Dia.
8,970 in/sec

(c) $V_f = 10\%$
.016 Wire Dia.
8,510 in/sec

(d) $V_f = 26\%$
.008 Wire Dia.
4,650 in/sec

(e) $V_f = 26\%$
.016 Wire Dia.
7,970 in/sec

(f) $V_f = 26\%$
.016 Wire Dia.
8,030 in/sec

(g) Fiberglass
5,400 in/sec

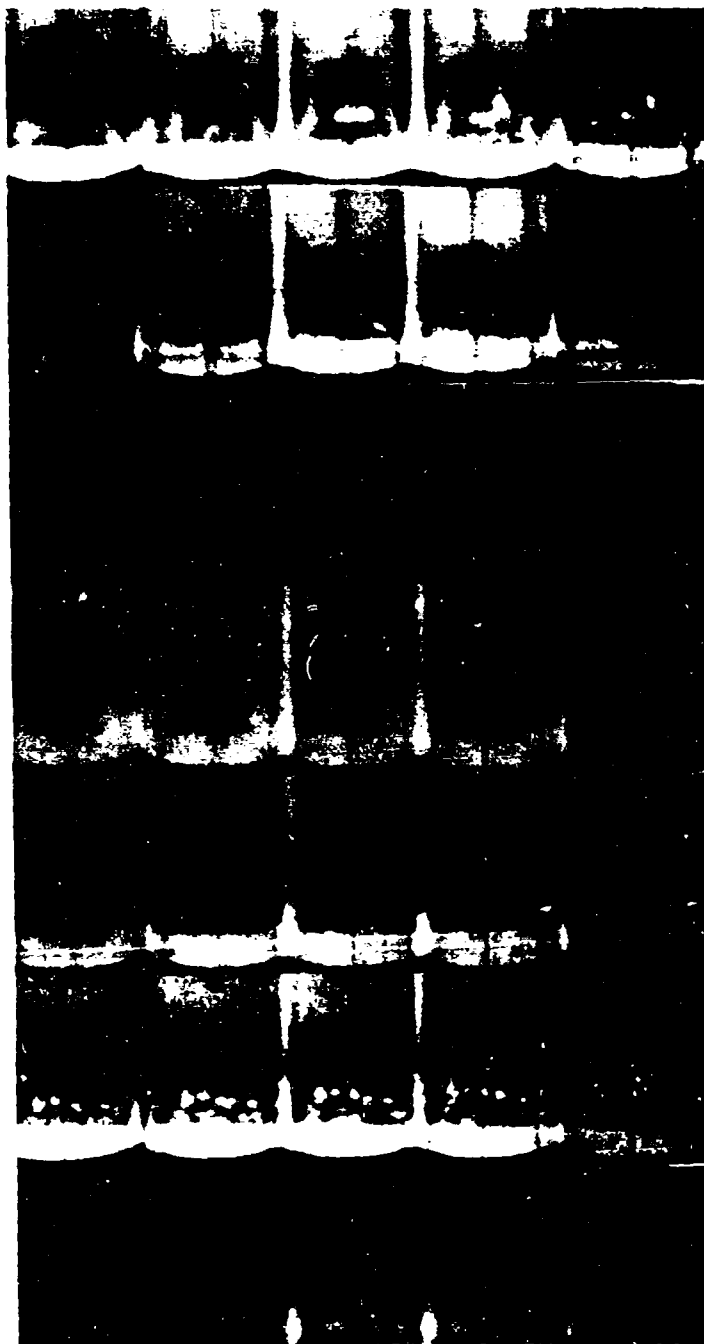


Figure 37. Dynamic Fracture Behavior of Composites

ALUMINUM-NICKEL COMPOSITES Velocity given in inches per second



2024-T4 ALUMINUM

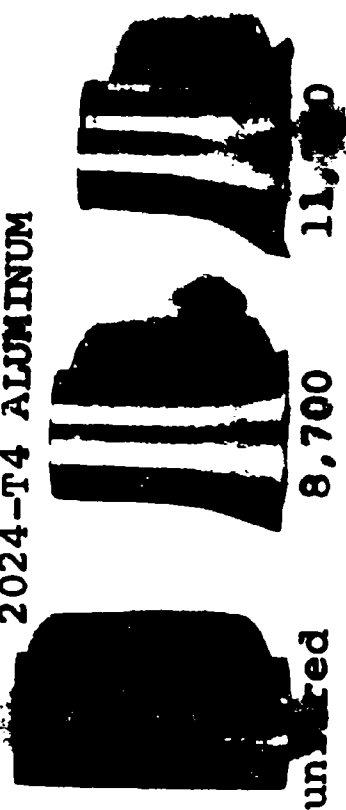


Figure 38. Aluminum-Nickel Composite Failure Behavior

SECTION V

CONCLUSIONS

The dynamic compressive properties of steel reinforced epoxy, fiberglass, reinforced polyester and aluminum-nickel reinforced aluminum have been investigated at various strain rates. These materials are representative of continuous and discontinuous reinforced composite systems in metal and non-metal matrices. The compressive test results for the laboratory prepared steel-epoxy specimens showed a high degree of reproducibility and consistency.

It has been demonstrated that for the materials tested, a greater degree of strain rate sensitivity is evidenced at the lower values $<10^0$ in/in/sec and less at the higher rates. In addition, an apparent transition region exists for the steel-epoxy specimens with increase in volume percent of filaments as a function of strain rate.

Further, distinct shear failure modes have been observed for the continuous and discontinuous filaments as a function of strain rate. For the steel-epoxy specimens a shear failure associated with filament micro-instability has been observed for some specimens. The apparently consistent mode of failure was associated with local filament buckling and matrix shear. The fiberglass specimens showed a distinct brush-like failure associated with the loaded end of the specimen. For the discontinuous aluminum nickel system, distinct localized shear failure accompanied by rotation and lateral slip of the reinforcing elements occurs.

Studies on the terminal ballistics problem have been made and results show the particular failure and fracture characteristics of the materials tested. An investigation of methods for predicting composite projectile failure from dynamic stress-strain diagrams has been demonstrated. Equating dynamic kinetic energy to stored energy obtained from Hopkinson Pressure Bar studies has yielded extremely good correlation between calculated and observed failure.

The results presented in this report certainly must be considered as preliminary; however, they do indicate the general nature of the dynamic failure characteristics of several representative composites and will serve as a basis for further studies designed to determine the suitability of composite materials for projectiles and other dynamic applications.

REFERENCES

1. Summary Report, "A Working Conference: Fundamental Problems of Future Aerospace Structures," AFOSR Report No. 67-2175, Air Force Office of Scientific Research (1967).
2. SAMPE Symposium on Filament Winding Conference, Pasadena California, March 28-30 (1961).
3. Holliday, L., "Composite Materials," Elsevier Publishing Company, London (1966).
4. SAMPE Symposium on Advanced Fibrous Reinforced Composites, San Diego, California, Nov. 9-11 (1966).
5. "Fiber Strengthened Metallic Composites," Symposium presented at the American Society for Metals, ASTM STP #427, November (1966).
6. "Metalmatrix Composites," ASTM Special Technical Publication No. 438, ASTM (1967).
7. Broutman, L. J. and Krock, R. H., "Modern Composite Materials," Addison-Wesley Publishing Co., Reading, Mass. (1968).
8. Tsai, S. W., Halpin, J. C. and Pagno, N. J., "Composite Materials Workshop," Technomic Publishing Co., Stamford, Conn. (1968).
9. Ashton, J. E., Halpin, J. C. and Petit, P. H., "Primer on Composite Materials: Analysis," Technomic Publishing Co., Stamford, Conn. (1969).
10. Editors of Materials and Design Engineering, "The Promise of Composites," Materials Engineering, Vol. 63, p. 79 September (1963).
11. Williams, R. V., "Progress in Composite Materials," Engineering Digest, Vol. 28, p. 67 (1967).
12. Kreider, K. G., Varholak, E., Breinan, E. and Schile, R. D., "Investigation of Plasma Sprayed Metal Matrix Fiber Reinforced," UCARL-FGL0541, December (1967).
13. Adamski, R., Bhattacharya, S. and Parikh, N. M., "Influence of Fabrication Variables on the Properties of Fiber Reinforced Metals," Report No. IITRI-B607406, IIT Research Institute, Chicago, Illinois, July (1968).

14. Calfee, J. D., et al., "Fabrication Techniques for High Performance Composite Materials," Report No. AD 488 380, Monsanto Research Corp., April (1967).
15. Jackson, S. M., et al., "Fiber-Reinforced Metal Matrix Composites," Report No. AD 824 631, Battelle Memorial Inst., September (1967).
16. Snide, J. A., et al., "Current Developments in Fiber-Reinforced Composites," Report No. AFM.-TR-67-359, Air Force Materials Lab, February (1968).
17. Simizu, H., Dolowy, J. F., Taylor, R. J. and Webb, B. A., "Metal Matrix Composites Behavior and Aerospace Applications," SAE TRANS, Vol. 76, p. 167 (1968).
18. Wolff, E. G. and Hill, R. J., "Evaluation of Fabrication Techniques for Metal Matrix Composites," J. Compos. Matls., Vol. 2, p. 405 (1968).
19. Thornton, H. R., Fabrication of Metal Matrix Composite Materials," J. Compos. Matls. Vol. 2, p. 32 (1968).
20. Alexander, J. A., "Five Ways to Fabricate Metal Matrix Composite Parts," Matls. Eng., Vol. 68, p. 58 (1968).
21. Compton, W. A. and Steward, K. P., "Compatibility Considerations for Metal Matrix Composites," SAE TRANS, Vol. 76, p. 161 (1968).
22. Joseph, E., Myers, E. J. and Stuhrike, W. F., "Diffusion Bonding and Testing of Boron-Aluminum Composites," J. COMPOS. MATLS. Vol. 2, p. 56, January (1968).
23. Jarvis, C. V., "Explosive Fabrication of Composite Materials," Nature, Vol. 220, p. 782 (1968).
24. Davies, G. F., and Baskey, R. H., "Titanium Alloy Wire-Reinforced Composites - A Progress Report," J. Metals, Vol 20, p. 80, August (1968).
25. Zdanuk, E. J. and Krock, R. H., "Application of Vacuum Processing to Tungsten-Copper Composites," Vacuum, Vol. 18, p. 464 (1968).
26. Lager, J. R. and June, R. R., "Design, Analysis, Fabrication and Test of a Boron Composite Beam," J. Compos. Matls. Vol. 2, p. 128 (1968).

27. Thompson, E. R. and Lemkey, F. D., "Aligned Eutectics: Tomorrow's Composites," Matls. Eng., Vol. 68, p. 58, September (1968).
28. Schwartz, H. S. and Spain, R. G., "Structural Plastic Composites Incorporating New High-Modulus Fibers," AIAA J., Vol 6, p. 1043 (1968).
29. Fleck, J. and Leonard, R., "High-Energy Techniques for Composite Fabrication - Explosive Consolidation," J. Metals, Vol. 21, p. 10A, March (1969).
30. Alexander, J. A., "The Fabrication of Rod Composite Forms in the Mg-B System," J. Metals, Vol. 21, p. March (1969).
31. Williford, J. F. Jr. and Snajdr, E. A., "Investigation of Fiber-Reinforced Metal Matrix Composites Using a High Energy-Rate Forming Method," J. Metals, Vol. 21, p. 10A, March (1969).
32. Hamilton, C. H., "Diffusion Bonded Titanium-Borsic Composites," J. Metals, Vol. 21, p. 25A, March, (1969).
33. Dolowy, J. F., "Fabrication and Processing Mechanisms Active in Al-B Composites," J. Metals, Vol. 21, p. 9A, March (1969).
34. McDanel, D. L., Jech, R. W. and Weeton, J. W., "Stress-Strain Behavior of Tungsten-Fiber-Reinforced Copper Composites," NASA TN D-1881, October (1963).
35. Vasilos, T. and Wolff, E. G., "Strength Properties of Fiber-Reinforced Composites," J. Metals, Vol. 18, p. 583, (1966).
36. Schwartz, H. S., et al., "Mechanical Behavior of Beryllium with Reinforced Plastic Composites. Part I. Static Mechanical Properties," Report No. AFML-TR-66-404, January (1967).
37. Symposium, "Testing Techniques for Filament Reinforced Plastics," Air Force Materials Lab., Wright Patterson AFB, Ohio, Sept. 21-23 (1966).
38. Friedman, Edward, "A Tensile Failure Mechanism for Whisker Reinforced Composites," Society of the Plastics Industry, Inc. (1967).
39. Bloom, J. M. and Wilson, H. B., Jr., "Axial Loading of a Unidirectional Composite," J. Compos. Matls., Vol. 1, p. 268 (1967).

40. Ivanova, V. S. and Ustinov, L. M., "Tensile Strength Diagrams for Composite Metals Containing Fibers," Russ. Met. R. No. 5, p. 63 (1967).
41. Lees, J. K., "A Study of the Tensile Modulus of Short Fiber-Reinforced Plastics," Polymer Eng. Sci. Vol. 8, p. 186 (1968).
42. Carrara, A. S. and McGarry, F. J., "Matrix and Interface Stresses in a Discontinuous Fiber Composite Model," J. Compos. Matls., Vol. 2, p. 222 (1968).
43. Chang, C. S. and Conway, H. D., "Bond Stresses in Fiber Reinforced Composites Subjected to Uniform Tension," J. Compos. Matls., Vol. 2, p. 168 (1968).
44. Davison, J. E. and Mahien, W. R., "Mechanical Behavior of a Wire Reinforced Aluminum Composite," J. Metals, Vol. 21, p. 38A, March (1969).
45. Zecca, A. R., Hay, D. R., and Krajewski, H. P., "Elastic Properties of Metal-Matrix Composites," J. Metals, Vol. 21, p. 38A, March (1969).
46. Ebert, L. J. and Fedor, R. J., "Effect of Mechanical Prestraining on Tensile Behavior of Metal-Matrix Composites," J. Metals, Vol. 21, p. 26A, March (1969).
47. Sippel, G. R., Tsareff, T. C., Jr., and Herman, M., "Strength Properties of Unidirectional B-Al and SiC-Ti Composites," J. Metals, Vol. 21, p. 25A, March (1969).
48. Moore, C., "Strength of Composite Materials Reinforced with Brittle Fibers," J. Metals, Vol. 21, p. 40A, March (1969).
49. Broutman, L. J., "Failure Mechanisms for Filament Reinforced Plastics," Modern Plastics, Vol. 42, p. 143 (1965).
50. Noyes, J. V., et al., "Crazing and Yielding of Reinforced Composites," Rept. No. DAC-33525, Douglas Aircraft Co., December (1966).
51. Gillman, J. W., et al., "Modes of Failure of Glass Fiber Reinforced Plastics under Compressive Loads," Rept. No. TAM-307, Illinois University, September (1967).
52. Steg, L., Rosen, B. W. and Sutton, W. H., "Fiber Reinforced Materials," Presented at the 7th International Symposium in Space Technology and Science, Tokyo, Japan (1967).

53. Herman, L. R., Mason, W. E. and Chan, S. T. K., "Response of Reinforcing Wires to Compressive States of Stress," J. Compos. Matls., Vol. 1, p. 211 (1967).
54. Bobeth, W., "Investigation on the Response of Fibers to Axial Compression," Faserforschung und Textiltechnik, Vol. 8, p. 547 (1967).
55. Achenbach, J. D., Herman, J. H. and Ziedler, F., "Tensile Failure of Interface Bonds in a Composite Body Subjected to Compressive Loads," AIAA J., Vol. 6, p. 2040 (1968).
56. Lager, J. R., and June, R. R., "Compressive Strength of Boron-Epoxy Composites," J. Compos. Matls., Vol. 3, p. 48 (1969).
57. Schapery, R. A., "Stress Analysis of Viscoelastic Composite Materials," J. Compos. Matls., Vol. 1, p. 228 (1967).
58. Ashton, J. E., "Non-Linear Viscoelastic Response of Fibrous Composites," J. Compos. Matls., Vol. 2, p. 116 (1968).
59. Lou, Y. C. and Schapery, R. A., "Viscoelastic Behavior of Fiber-Reinforced Composite Materials," Rept. No. AD-681 136, Purdue University, Lafayette, Indiana, April (1968).
60. Hashin, Z. et al., "Static and Dynamic Viscoelastic Behavior of Fiber Reinforced Materials and Structures," Rept. No. AD-680 285, Franklin Inst. Research Labs., Phila. Pa., 136 p. (1968).
61. Nicolas, T., "The Mechanics of Ballistic Impact - A Survey," AFML-TR-67-208, July (1967).
62. Ewing, W. M., Jardetzky, W. S. and Press, F., "Elastic Waves in Layered Media," McGraw Hill Book Co., (1957).
63. Eason, G., "Wave Propagation in Inhomogeneous Elastic Media," Bulletin of the Seismological Society of America, Vol. 57, p. 1267 (1967).
64. Sinha, N. K., "Propagation of Love Type Waves in a Non-Homogeneous Layer Lying Over a Vertically Semi-Infinite Homogeneous Isotropic Medium," Pur. A. Geoph., Vol. 73, p. 47 (1969).
65. Bhattach, J., "On Propagation of Certain Types of Surface Waves in a Non-Homogeneous Elastic Layer," Pur. A. Geoph. Vol. 73, p. 93 (1969).

66. Kinslow, R., "Stress Waves in Composites Laminates," Rept. No. Ad 465 129, Arnold Engineering Development Center, Tenn. June (1965).
67. Brepta, R., "Wave Propagation in Laminated Elastic Materials," Strojnicky Casopis (in Czech), Vol. 16, p. 545 (1965).
68. Chou, S. C., et al., "Numerical Solution of Stress Waves and Layered Media," AIAA J., Vol. 6, p. 1067 (1968).
69. Lindholm, U. S. and Doshi, K. D., "Wave Propagation in an Elastic Nonhomogeneous Bar of Finite Length," J. Appl. Mech. Vol. 32, p. 135 (1965).
70. Payton, R. G., "Elastic Wave Propagation in a Non-Homogeneous Rod," Qrtly. J. Mech. Appl. Math., Vol. 19, p. 83 (1966).
71. Achenbach, J. D., "Wave Propagation in Lamellar Composite Materials," J. Acous. Soc. Vol. 43, p. 1451 (1968).
72. Reddy, D. P., "Stress Waves in Nonhomogeneous Elastic Rods," J. Acous. Soc., Vol. 34, p. 1273, (1969).
73. Hsu, H. P., "Wave Propagation in Anisotropic Media," M. Tens. Q., Vol. 19, p. 47 (1968).
74. Sneddon, I. N. and Hill, R., "Elastic Waves in Anisotropic Media," Progress in Solid Mechanics, Chapter II, North Holland Publishing Company, Amsterdam, (1961).
75. Cameron, N. and Eason, G., "Wave Propagation in an Infinite Transversely Isotropic Elastic Solid," Quart. Journ. Mech. Appl. Math., Vol. 20, p. 23 (1967).
76. Achenbach, J. D. and Hermann, G., "Dispersion of Free Harmonic Waves in Fiber-Reinforced Composites," AIAA J., Vol. 6, p. 1832 (1968).
77. Chou, P. C., "Introduction of Wave Propagation in Composite Materials," in Composite Materials Workshop, Technomic Publishing Co., Stamford, Conn. (1968).
78. McNiven, H. D. and Mergi, Y., "Controlled Dispersion of Axisymmetric Waves in Composite Rods," J. Acous. Soc., Vol. 43, p. 691 (1968).

79. Kenner, V. H. and Goldsmith, W., "One Dimensional Wave Propagation Through a Short Discontinuity," J. Acous. Soc., Vol. 45, p. 115 (1969).
80. "Behavior of Materials under Dynamic Loading," ASME Publication (1965).
81. "Designing for High Impact Technology," ASME Publication (1965).
82. Lindholm, U. H., "Mechanical Behavior of Materials Under Dynamic Loads," Springer-Verlag, Berlin (1968).
83. Kolsky, H., "An Investigation of the Mechanical Properties of Materials at Very High Rates of Loading," Proc. Phys. Soc., Vol. 62B, p. 676 (1949).
84. Chiddester, J. L. and Malvern, L. E., "Compression-Impact Testing of Aluminum at Elevated Temperatures," Exp. Mech., Vol. 3, p. 81 (1963).
85. Davies, E. D. H. and Hunter, S. C., "The Dynamic Compression Testing of Solids by the Method of the Split Hopkinson Pressure Bar," J. Mech. Phys. Sol., Vol. 11, p. 155 (1963).
86. Lindholm, U. S., "Some Experiments with the Split Hopkinson Pressure Bar," J. Mech. Phys. Sol., Vol. 12, p. 317 (1964).
87. Lindholm, U. S. and Yeakley, L. M., "High Strain Rate Testing, Tension and Compression," Experimental Mechanics, Vol. 8, p. 1 (1968).
88. Chiu, S. S. and Neubert, V. H., "Difference Method for Wave Analysis of the Split Hopkinson Pressure Bar With Viscoelastic Specimen," J. Mech. Phys. Sol., Vol. 15, p. 177 (1967).
89. Nevill, G. E., Jr., Loyd, J. M. and Fuehrer, H. R., "Dynamic Properties of Metal Powder Epoxy Resin Composites," J. Compos. Matls., Vol. 3, p. 174 (1969).
90. Tarcliff, H. P. and Marquis, H., "Some Dynamic Properties of Plastics," Canadian Aero. and Sp. J., Vol. 9, p. 295 (1963).
91. Tsai, S. W., "Some Observations on the Dynamic Behavior of Composites," Monsanto Research Corp., St. Louis, Mo., Sept. (1968).
92. Abbott, B.W. and Broutman, L.J., "Stress-Wave Propagation in Composite Materials," Experimental Mech., Vol. 6, p. 383 (1966).

93. Sharma, M. G., Critchfield, M. and Lawrence, W. F., "Dynamic Mechanical Studies of a Composite Material," Shock and Vibration Bulletin, Naval Research Laboratory, No. 36, p. 95 (1967).
94. Behrens, E., "Dynamic Testing of Composite Materials," Text. Res. J., Vol. 38, p. 1075 (1968).
95. Behrens, E., "Elastic Constants of Composite Materials," J. Acoust. Soc., Vol. 45, p. 102 (1969).
96. Behrens, E. and Kremhell, A., "Wave Propagation in Composites and Average Material Constants," Non-Destr. Test., Vol. 2, p. 55, (1969).
97. Kolsky, H., Stress Waves in Solids, Clarendon Press, Oxford (1953).
98. Rinehart, J. S. and Pearson, J., Behavior of Metals under Impulsive Loads, American Society of Metals, Cleveland (1954).
99. Goldsmith, W., Impact, Edward Arnold, London (1960).
100. Symposium on Dynamic Behavior of Materials; ASTM Special Technical Publication No. 336, ASTM (1963).
101. Kelly, A. and Tyson, W. R., "Tensile Properties of Fiber-Reinforced Metals: Copper/Tungsten and Copper/Molybdenum," J. Mech. Phys. Sol., Vol. 13, p. 329 (1965).
102. McGarry, F. J., "Relationships Between Resin Fracture and Composite Properties," Rept. No. AFM-TR-66-288, MIT, Sept. (1966).
103. Cooper, G. A. and Kelly, A., "Tensile Properties of Fiber Reinforced Metals: Fracture Mechanics," J. Mech. Phys. Sol., Vol. 15, p. 279 (1967).
104. Outwater, J. O., et. al., "The Fracture Energy of Composite Materials," Rept. No. AD 659 363, Vermont University, August (1967).
105. Zweden, C. "Tensile Failure of Fiber Composites," AIAA J. Vol. 6, p. 2325, (1968).
106. Mullin, J., Berry, J. M. and Gotti, A., "Some Fundamental Fracture Mechanisms Applicable to Advanced Filament Reinforced Composites," J. Compos. Matls. Vol. 2, p. 82 (1968).

107. Vanderveldt, H. and Liebowitz, H., "Carrying Capacity and Fracture Mechanisms Applicable to Advanced Filament Reinforced Composites," J. Compos. Matls., Vol. 2, p. 82 (1968).
108. McKee, R. B. and Sires, G., "A Statistical Model for Tensile Fracture of Parallel Fiber Composites," ASME Technical Paper WA/RP-7 (1969).
109. Jones, R. L. and Cooke, F. W., "Roll Bonded Beryllium- Aluminum Lamellar Composites," J. Metals, Vol. 21, p. 10A, March (1969).
110. Gupta, B. P., and Davids, N., "Penetration Experiments with Fiberglass Reinforced Plastics," Experimental Mechanics, Vol. 6 p. 445 (1966).
111. Mettes, D. G., "Glass Fiber Reinforced Plastic Personnel Armor," Rept. No. AD 918 564, Owens Corning Fiberglass Corp., November (1964).
112. Alessi, A. L. and Barron, E. R., "Plastic-Ceramic Composite Armor," J. Soc. Pl. Eng., Vol. 24, p. 19 (1969).
113. Wilkins, M. L., "Armor Penetration Phenomena," Presented at the Third Symposium on Lightweight Armor Materials, Cleveland, Ohio, August 13-15 (1968).
114. Valentine, R. H., "A Study of Composites in Light Armor Systems," Presented at the 4th Annual Symposium of High Performance Composites, St. Louis, Mo., April (1969).
115. Dunleavy, J. G., Bodine, E. G. and Rolsten, R. F., "Significance of Dynamic Material Response in Ceramic Armor Design," Bull. Am. Ceramic Soc., Vol. 41, No. 4, p. 488 (1969).
116. Cline, C. F., Wilkins, M. L., "Importance of Material Properties in Ceramic Armor," Bull. Am. Ceramic Soc., Vol. 48, No. 4, p. 487 (1969).
117. Bailey, W. O. and Miccioli, B. R., "Ballistic Defeat as a Function of Some Ceramic Properties," Bull. Am. Ceramic Soc., Vol. 28, No. 4, p. 487 (1969).
118. Johnson, P. C., Haggerty, J. S., Davis, R. S., "Interaction of Ductile Projectiles with Ceramic Armor," Bull. Am. Ceramic Soc., Vol. 48, No. 4, p. 486 (1969).

119. Frechette, V. D. and Cline, C. F., "Fractography of Ballistically Tested Ceramics," Bull. Am. Ceramic Soc., Vol. 48, No. 4, p. 486 (1969).
120. Torti, M. L. and Newell, C. R., "Probability of Penetration of Ceramic Armor as a Function of Velocity," Bull. Am. Ceramic Soc., Vol. 48, No. 4, p. 486 (1969).
121. Steverding, B., "Theory of Ballistic Protection by Brittle Materials," Bull. Am. Ceramic Soc., Vol. 48, No. 4, p. 487 (1969).
122. O'Shea, R. P. and Watmough, T., "Application of Ceramic Materials for Armor Systems," Bull. Am. Ceramic Soc., Vol. 48 No. 4, p. 488 (1969).
123. Green, S. J., Schierloh, F. L., Perkins, R. D., and Babcock, S. G., "High Velocity Deformation Properties of Polyurethane Forms," Experimental Mechanics, Vol. 9, p. 103 (1969).
124. Stepka, F. S., "Projectile-Impact-Induced Fracture of Liquid-Filled, Filament Reinforced Plastic or Aluminum Tanks," Report No. NASA TN D-3456 (1966).
125. McMillan, A. R., Diedrich, J. H., and Clough, N., "Hyper-velocity Impacts into Stainless-Steel Tubes Armored with Reinforced Beryllium," Report No. NASA TN D-3512 (1966).
126. Godfrey, D. E., "Equipment Design for Investigation of Plastic Deformation of Plates," Masters Thesis, Dept. of Aeronautical Engineering, U. of Minnesota, Dec. (1967).
127. Lemkey, F., Hertberg, R. and Ford, J., "The Microstructure, Crystallagraphy, and Mechanical Behavior of Unidirectionally Solidified Al-Al₃Ni Eutectic," Vol. 233, 1965, pp. 334-341.

UNCLASSIFIED

Security Classification

DOCUMENT CONTROL DATA - R & D		
<i>(Security classification of title, body of abstract and indexing annotation must be entered when the overall report is classified)</i>		
1. ORIGINATING ACTIVITY (Corporate author) Department of Engineering Science and Mechanics University of Florida Gainesville, Florida		2a. REPORT SECURITY CLASSIFICATION Unclassified 2b. GROUP
3. REPORT TITLE STUDIES ON THE BALLISTIC IMPACT OF COMPOSITE MATERIALS		
4. DESCRIPTIVE NOTES (Type of report and inclusive dates) Final Report 17 June 1968 to 16 June 1969		
5. AUTHOR(S) (First name, middle initial, last name) R. L. Sierakowski C. A. Ross G. E. Nevill, Jr. E. R. Jones		
6. REPORT DATE July 1969	7a. TOTAL NO. OF PAGES 85	7b. NO. OF REFS 126
8a. CONTRACT OR GRANT NO. FO8635-68-C-0115 b. PROJECT NO. c. d.	9a. ORIGINATOR'S REPORT NUMBER(S) 9b. OTHER REPORT NO(S) (Any other numbers that may be assigned this report) AFATL-TR-69-99	
10. DISTRIBUTION STATEMENT This document is subject to special export controls and each transmittal to foreign governments or foreign nationals may be made only with prior approval of the Air Force Armament Laboratory, (ATRD), Eglin AFB, Florida 32542.		
11. SUPPLEMENTARY NOTES Available in D D C		12. SPONSORING MILITARY ACTIVITY Air Force Armament Laboratory Air Force Systems Command Eglin Air Force Base, Florida
13. ABSTRACT The dynamic compressive behavior of unidirectional composites consisting of representative continuous and discontinuous filament reinforced specimens has been investigated. Principal emphasis has been placed on a steel-epoxy system for which a fabrication procedure yielding specimens of high quality and consistency has been developed. Tests at various strain rates were conducted using a conventional Tinius Olsen machine and a Split Hopkinson Pressure Bar System. Results indicating the influence of volume fraction of reinforcing material in the steel-epoxy specimens on strain rate sensitivity are obtained. The apparent existence of a transition region in strain rate sensitivity as the volume percent of reinforcement increased has been noted. Evidence has also been obtained on the mode of failure for the steel-epoxy specimens as a function of strain rate and volume percent of reinforcement. For the Al-Al ₃ Ni specimens a shear mode failure based on rotation and lateral motion of the 'discontinuous' reinforcements was observed while the fiberglass specimens exhibited a brush-like failure. The failure characteristics of composites under low velocity impact were studied using an air gun assembly developed under this program. A simple method of predicting failure modes and critical velocities from the strain rate data is proposed for the steel-epoxy specimens. Comparisons of the theoretical predictions with experimental results show good agreement. Further correlation of the terminal ballistics behavior of composite projectiles with their dynamic properties has been obtained from photographic recordings of the impact event.		

DD FORM 1473
1 NOV 65

UNCLASSIFIED

Security Classification

UNCLASSIFIED

Security Classification

14. KEY WORDS	LINK A		LINK B		LINK C	
	ROLE	WT	ROLE	WT	ROLE	WT
Dynamic Compressive Behavior						
Unidirectional Composites						
Filament Reinforced						
Strain rates						
Failure modes						
Critical velocities						

UNCLASSIFIED

Security Classification